# Spatio-temporal patterns and drivers of terrestrial Dissolved Organic Carbon (DOC) leaching to the European river network.

Céline Gommet[1,3], Ronny Lauerwald[2], Philippe Ciais[3], Bertrand Guenet[4], Haicheng Zhang[1], Pierre Regnier[1]

[1]Biogeochemistry and Earth System Modelling, Department of Geoscience, Environment and Society, Universite Libre de Bruxelles, Bruxelles, Belgium
[2]Université Paris-Saclay, INRAE, AgroParisTech, UMR ECOSYS, 78850, Thiverval-Grignon, France
[3]Laboratoire des Sciences du Climat et de l'Environnement, UMR8212, CEA-CNRS-UVSQ F-91191 Gif sur Yvette, France
[4]Laboratoire de Géologie, UMR 8538, Ecole Normale Supérieure, IPSL, PSL Research University, CNRS, Paris, France

*Correspondence to*: Céline Gommet (celine.gommet@ulb.be)

**Abstract.** Leaching of dissolved organic carbon (DOC) from soils to the river network is an important component of the land carbon (C) budget. At regional to global scales, its significance has been estimated through simple mass budgets, often using multi-year averages of observed fluvial DOC fluxes as proxy of DOC leaching due to the limited availability of observations of the leaching flux itself. This procedure leads to a systematic underestimation of the leaching flux because of the decay of DOC during fluvial transport. Moreover, this procedure does not allow revealing spatio-temporal variability in DOC leaching from soils, which is vital to better understand the drivers of DOC leaching and its impact on the local soil C budget. In this study, we use the land surface model ORCHILEAK to simulate the terrestrial C budget including leaching of DOC from the soil and its subsequent reactive transport through the river network of Europe. The model performance is evaluated not only against the sparse observations of soil DOC leaching rate, but also against the more abundant observations of fluxes and reactivity of DOC in rivers, providing further evidence that our simulated DOC fluxes are realistic. The model is then used to simulate the spatio-temporal patterns of DOC leaching across Europe over the period 1972–2012, quantifying both the environmental drivers of these patterns as well as the impact of DOC leaching on the land C budget. Over the simulation period, we find that, on average, 14.3 TgC yr$^{-1}$ of DOC is leached from land to European rivers, which is about 0.6% of the terrestrial net primary production, a fraction significantly lower than that reported for tropical river networks. On average, 12.3 TgC yr$^{-1}$ of the leached DOC is finally exported to the coast via the river network, and the rest is respired during transit. DOC leaching presents a large seasonal variability, with the maximum occurring in winter and the minimum in summer, except for most part of the Northern Europe where the maximum occurs in spring due to the snow melt. DOC leaching rate is generally low in warm and dry regions, and high in cold and wet regions of Europe. Furthermore, runoff, and the ratio between runoff from shallower flow paths vs. deep drainage and groundwater flow, are the main drivers of the spatio-temporal variation of DOC leaching. Temperature, as a major control of DOC production and decomposition rates in the soils, plays only a secondary role.

## 1 Introduction

Terrestrial ecosystems are an important carbon (C) sink as they absorb about one fourth of anthropogenic $CO_2$ emissions and store these C in plant biomass and soil carbon pools (Friedlingstein et al., 2020). This terrestrial C sink mitigates the growth rate of atmospheric $CO_2$ concentration and thus plays an important role in regulating climate change (Ciais et al., 2013). However, the efficiency of that sink is partly alleviated by the permanent, lateral leaching of C from soils, through the river network down to the ocean (Regnier et al., 2013). An accurate understanding of lateral C fluxes through the river network is thus necessary to better understand the global C cycling and to inform policies of climate change mitigation (Le Quéré et al., 2018).

The identification of riverine C transfers as a key component of the continental C budget constituted an important paradigm shift in our understanding of the global C cycle (Cole et al., 2007). More recently, riverine C cycling was also shown to be affected by anthropogenic perturbation and thus to be an element of the anthropogenic $CO_2$ budget (Regnier et al., 2013; Le Quéré et al. 2015). Anthropogenic perturbations of riverine C fluxes are manifold and comprise direct impacts through changing C and nutrient inputs following land-use change and agricultural activities, wastewater discharge, and hydraulic management (e.g. Tian et al., 2015; Lauerwald et al., 2020; Hastie et al., 2021; Maavara et al., 2017). There are also indirect impacts following climate change and changes in atmospheric composition. Together, these perturbations have accelerated the turnover of C along the terrestrial-inland water continuum. The terrestrial C sink, which is classically estimated without taking into account the C exports through the river network, is thus generally overestimated (Regnier et al., 2013; Lauerwald et al., 2020).

The integration of riverine C transfers into the terrestrial C budget requires the quantification of the amount of C lost from soils to the river network. Due to the scarcity of observational data, this flux is not easy to estimate based on empirical methods. At global scale, this flux was constrained through budget closure based on estimates of riverine C exports to the coast, and estimates of C losses to the atmosphere and aquatic sediments during transport. The existing global estimates of these soil C exports to the river network, as synthesized by Drake et al. (2018), range from 1.1 to 5.1 PgC $yr^{-1}$ – a huge uncertainty range reflecting the limitations of empirical estimation approaches and the paucity of underlying data. Over the past decade, a new generation of land surface models (LSMs) have been developed, which represent the export of C from soils to the river network, and in some cases even the transport and cycling of these terrestrial C loads along the river network down to the coast (Smith et al. 2010; Kicklighter et al. 2013; Tian et al., 2015; Lauerwald et al., 2017; Nakhavali et al., 2018). With the exception of the study by Tian et al. (2015), all these studies focus on the lateral export of dissolved organic C (DOC) which is a product of the incomplete decomposition of plant litter and soil organic carbon (SOC). These mechanistically based models allow to predict the leaching of DOC in unmonitored regions and to assess the spatial and temporal variability which, to date, can only be poorly resolved by empirical methods. Moreover, these approaches link the C exports from soils to the river network to the terrestrial C cycle, and thus allow to directly assess the role of these C exports on the terrestrial C budget, its perturbation through changes in land use, climate and atmospheric chemistry, and its impact on the terrestrial sink for anthropogenic $CO_2$ emissions.

75    In this study, we use the LSM ORCHILEAK (Lauerwald et al. 2017), a branch of the IPSL-LSCE LSM

76    ORCHIDEE (Krinner et al. 2005), to quantify the DOC leaching from soils and its effects on the terrestrial C

77    budget in Europe. ORCHILEAK not only simulates the vertical C cycling between vegetation, soils and

78    atmosphere in response to climate, atmospheric $CO_2$ concentrations, and land use change, but also represents the

79    lateral exports of DOC from soils to the river network as well as the reactive transport of that DOC through the

80    river network. To our knowledge, only one study (Kindler et al., 2011) has estimated the soil DOC leaching flux

81    based on runoff and direct observations of DOC concentrations in the soil water for various locations across

82    Europe. Thus, this empirical assessment will be used for evaluating the simulated DOC leaching fluxes in this

83    study. Further, we evaluate simulated against observed riverine DOC fluxes, which are obtained from different

84    water quality surveys and scientific publications. Assuming a realistic representation of DOC reactivity in the

85    river network, which is to be evaluated against observations as well, this model-data comparison of riverine

86    DOC fluxes represents a valuable and additional possibility to assess the validity of simulated soil DOC

87    leaching.

88    So far, ORCHILEAK has been successfully tested and applied on large, near-natural river systems such as the

89    Amazon (Lauerwald et al. 2017, Hastie et al. 2019, Lauerwald et al. 2020), the Congo (Hastie et al. 2021) and

90    the Lena Rivers with a version also including some specific permafrost related mechanisms (Bowring et al.

91    2019, 2020). In this study, for the first time, ORCHILEAK is applied to, and evaluated for, the European river

92    network which is subject to direct impacts of agricultural land use, in contrast to more natural river basins. For

93    this reason, we devote special attention to manure application as an anthropogenic non-point source of DOC to

94    the river network, while we assume that for the period of simulation (1979-2012), due to the quality of sewage

95    water treatment, anthropogenic point sources of DOC are now negligible for most parts of Europe. Moreover, as

96    shown for instance by Meybeck (1986), DOC from sewage is highly labile and only affects concentration within

97    short distances downstream of water processing plants. Avoiding observational data from sites that are known to

98    be directly impacted by sewage inputs, we are able to evaluate model performance with regard to fluvial

99    transfers of soil derived DOC, which is the focus of our study.

100    Making full use of the capabilities of the ORCHILEAK model, we study in detail the spatio-temporal patterns in

101    DOC leaching and its quantitative contribution to the terrestrial C budget across Europe. We investigate how

102    specific climate zones in Europe differ with regard to seasonality in DOC leaching fluxes, which are

103    hypothesized to be controlled by hydrology, litter fall and temperature effects on litter and SOC decomposition.

104    We will further try to quantify the effect of these controls in the different climate zones of Europe. Finally, we

105    strive to find out in which climate zone DOC leaching affects the terrestrial C budget the most.

**2 Methodology**

**2.1 ORCHILEAK**

**2.1.1 Model overview**

ORCHILEAK (Lauerwald et al., 2017) is a branch of the model ORCHIDEE (Organizing Carbon and Hydrology in Dynamic Ecosystems) (Krinner et al., 2005), the land surface component of the Institut Pierre-Simon Laplace (IPSL) Earth system model (ESM). ORCHIDEE simulates energy, water and C fluxes between the atmosphere and the land at a global scale. This LSM is based on four sub-modules. The first one, SECHIBA, simulates the energy budget (energy, carbon and water) between the atmosphere and the biosphere as well as the hydrology, which in the default set-up used here, are both represented using a 30 minute time-step. The second sub-module, adapted from the LPJ model (Sitch et al., 2003), represents the dynamics of vegetation distribution on long time scales (1 year), while the third one (STOMATE) simulates the C dynamics in vegetation and soils at a daily to sub-daily step (Krinner et al., 2005). Finally, the fourth sub-module handles the routing of water that is lost via surface runoff and drainage from soils to the ocean through the global river network (Polcher 2003, Guimberteau et al., 2012), for which a daily time-step is used. All processes are simulated on a horizontal model grid, the resolution of which can be adapted to that of the meteorological forcing files. In this study, simulations are run at a spatial resolution of 0.5°. Moreover, in the default set-up, up to 13 plant function types (PFTs; bare soil, eight types of forest, two types of grassland and two types of cropland) can be distinguished for each cell, for which C budgets are simulated individually, while energy and water budgets are simulated at the grid cell level.

ORCHIDEE represents the soil C dynamics distinguishing different pools of plant litter and soil organic C over a 2 m profile. A branch of ORCHIDEE, called ORCHIDEE-SOM (Camino et al. 2018), added a vertical discretization of these carbon pools over 11 layers and included the representation of DOC production and cycling within the soil column (see section 2.1.2 for more details). ORCHILEAK was built on this branch and accounts for the coupled reactive transport processes impacting the dissolved C inputs from soils to the river network, including both DOC leaching from soils and $CO_2$ produced by soil respiration, into the hydrologic routing scheme. Besides advective transport of carbon with the water flow, ORCHILEAK simulates the decomposition of DOC during riverine transport, the gas exchange of $CO_2$ at the interface between the inland water and the atmosphere, and the exchange of C between water column and soil column in inundated floodplains. For the representation of in-river DOC decomposition, two pools with different decay rates are distinguished, a slow (refractory DOC) and a fast (labile DOC) pool. All those fluxes are closely coupled to the model representation of hydrology that comprises interception of precipitation, throughfall, infiltration, percolation, surface runoff, drainage, and the routing of discharge along the river-floodplain network.

 **2.1.2 Soil carbon module**

The soil carbon module of ORCHILEAK (Fig. 1) is derived from the CENTURY soil carbon model of Parton et al. (1988). In the standard scheme (Krinner et al., 2005), C in the soil of each model grid cell, and for each PFT, is represented by four different litter and three different soil organic carbon (SOC) pools with different turnover rates. The four litter pools correspond to metabolic aboveground and belowground litter, structural aboveground and belowground litter (Fig. 1). The SOC is subdivided into active, slow and passive pools, which have different default decomposition rates that are further modified at each time-step according to the evolving soil moisture and soil temperature. In the CENTURY scheme, C from the decomposed structural litter enters the active and the slow pools with the fraction allocated to each pools depending on lignin content of the litter, while the entire metabolic litter pool and the remaining part of structural litter is allocated to the active SOC pool. The SOC pools then feed into each other with the main C flux going from active to slow and passive to represent microbial decomposition of detrital organic matter, and a small return flux of slow and passive C back to the active pool to represent implicitly the C supply in the form of dead microbial biomass.
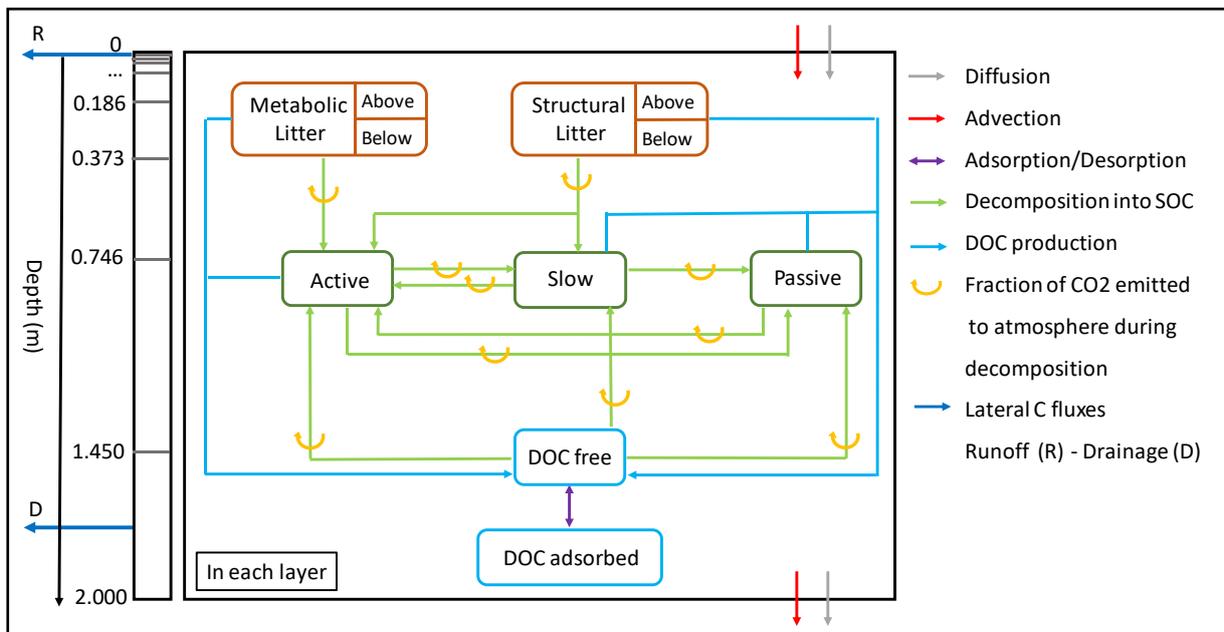
**Figure 1. The new version of the soil module of ORCHIDEE-SOM. The left box represents the discretization of the soil column and the transport processes between layers. The right box is a zoom of all the biogeochemical transformation processes that occur in each layer.**

Camino et al. (2018) updated this scheme with a vertical discretization of distinct SOC and litter pools over a 2 m soil profile represented by 11 layers, with geometrically increasing thickness from top to bottom (Figure 1). Camino et al. (2018) further developed the soil C module by including an explicit representation of the fate of DOC along this vertically discretized soil profile. Processes accounted for are DOC production from the decomposition of SOC and litter, decomposition of DOC within the soil, sorption/desorption of DOC onto/from mineral surfaces, vertical advection and diffusion of DOC through the soil column, and lateral, advective

164  leaching of DOC out of the soil profile, along with surface runoff (water flux from the topsoil surface) and

165  drainage (water flux from the last layer soil at 2m depth). In each soil layer, ORCHILEAK explicitly simulates

166  the fresh litter input (depending on the simulated vertical root distribution), decomposition of each organic

167  matter pool (including litter and SOC), C transformation between different organic matter pools (showed by blue

168  and green arrows between different pools in Fig. 1), C transport and diffusion between neighboring soil layers,

169  and the loss of DOC due to leaching. For a specific organic C pool at each time step, only a fraction of the

170  decayed C is respired as $CO_2$ to the atmosphere (orange arrows in Fig. 1), the remaining being transferred to

171  other organic pools (to mimic microbial growth and mortality).

172  The DOC dynamics in the soil are simulated according to equation (1), which accounts for the dynamic interplay

173  between production, decomposition, transport and sorption-/desorption processes along the discretized 2 m soil

174  column. All processes are simulated using a 30-minute time-step in following order: Firstly, production and

175  decomposition of DOC are calculated, and DOC stocks for each layer and pool are updated accordingly.

176  Secondly, vertical exchange of DOC between soil layers is simulated in two steps, first for the process of DOC

177  advection with the flow of water through the soil column, then for diffusion of DOC. Lastly, the export of DOC

178  through leaching from top- and bottom soil with runoff and drainage, respectively, are calculated.

179

$$\frac{dDOC_i}{dt} = \sum (Production_i - Decomposition_i) + F_{A,i} + F_{D,i} \tag{1}$$

180  In equation (1), $i$ stands for the index of each layer. Each layer is connected to the adjacent layers by advective

181  ($F_A$) and diffusive ($F_D$) fluxes. The total DOC transport flux is made of an advective component (equation 2)

182  computed as the product of the water flux $Q$ and the concentration of free DOC in the water solution of the $i^{th}$

183  layer and a diffusive component that follows Fick's first law (equation 3):

$$F_A = Q * DOC_i \tag{2}$$

$$F_D = -D * \frac{\partial^2 DOC}{\partial z^2} \tag{3}$$

184  where i stands for the ith layer, $z$ is the depth along the discretized soil profile, and $D$ stands for the molecular

185  diffusion coefficient of DOC, which is is assigned a value of $1.06 \times 10^{-5}$ m² d⁻¹ (Ota et al., 2013).

186  The advective export of DOC to the river network is proportional to the top (first five layers, 4.5 cm) and bottom

187  (11th layer) DOC concentrations, corresponding to water loss fluxes associated to runoff (for near surface) and

188  drainage (for deep soil layer). Diffusion of DOC between adjacent soil layers is proportional to the gradient in

189  DOC concentrations in the soil solution (eq. 3), moving towards an equilibrium. In addition, we apply a Fickian-

190  type transport to represent the effect of bioturbation on SOC profiles. In this case, the transport is represented

191  similar to eq. 3, but follows the gradient in SOC concentration relative to the volume of the soil layer.
192  Representing bioturbation as a diffusion-like process is a common approach in LSMs with vertically discretized
193  SOC scheme (Camino et al., 2018). However, bioturbation is much slower than diffusion of DOC in the soil
194  solution, with a diffusion coefficient D = 2.74x10$^{-7}$ m$^2$ d$^{-1}$ (Koven et al. 2013), compared to D=1.06x10$^{-5}$ m² d$^{-1}$
195  (Ota et al., 2013). Therefore, bioturbation impacts the vertical SOC profile while it has only a marginal influence
196  on the DOC dynamics. The right hand-side of Fig. 1 summarizes the set of production/decomposition processes
197  that occur in each layer. During litter decomposition, a fraction of the C is directly emitted back to the
198  atmosphere as $CO_2$ while the remainder feeds the active and slow SOC pools:
199

$$CO_2 \ respiration(Litter) = (1 - CUE) * k_L * (1 - \omega_L) * Litter \qquad (4)$$

$$Litter \ decomposition = CUE * k_L * (1 - \omega_L) * Litter \qquad (5)$$

200  where $k_L$ is the kinetic rate for the litter decomposition (dependent on soil moisture and temperature (Camino et
201  al., 2018)) and $\omega_L$ the fraction of litter that is channelled into DOC production (as opposed to particulate SOC).
202  This approach of relating DOC production directly to the decomposing litter is inspired by Nakhavali et al.
203  (2018) (following the ECOSSE model (Smith et al., 2010)) and is a major modification compared to the
204  previous version of soil DOC and POC cycling from Camino et al., 2018. In Eqs. (4) and (5), the partitioning
205  between SOC production and respiration is defined by the carbon use efficiency (CUE).
206  In turn, active SOC is degraded into both slow and passive SOC and the respiration fluxes associated with these
207  processes are also controlled by the CUE (Eqs. 6 and 7, with $k_{SOC}$ as the kinetic rate for SOC decomposition,
208  which depends on soil moisture and soil temperature, and $\omega_{SOC}$ as the fraction of decomposed SOC that is
209  transformed into DOC):
210

$$CO_2 \ respiration(SOC) = (1 - CUE) * k_{SOC} * (1 - \omega_{SOC}) * SOC \qquad (6)$$

$$SOC \ decomposition = CUE * k_{SOC} * (1 - \omega_{SOC}) * SOC \qquad (7)$$

211

212  The decomposition of the litter and SOC pools produces a small amount of DOC according to equation 8. The
213  DOC pool is thus fed by seven contributing sources, one for each of the four decomposing litter pools and three
214  from the decomposing SOC pools:
215

$$DOC \ production = k_L * \omega_L * Litter + k_{SOC} * \omega_{SOC} * SOC \qquad (8)$$

216  In ORCHIDEE-SOM (Camino et al. 2018), all decomposed litter and SOC which is not respired as $CO_2$, was
217  first fed into the DOC pools, and only upon the decomposition of that DOC, the non-respired fraction of the
218  decomposed DOC could feed the other SOC pools. Such formulation is in contrast to the adaption of the RothC
219  SOC model in ECOSSE (Smith et al., 2010) and JULES (Nakhavali et al., 2018) that we followed here, where

220     the major exchange of C is between the different litter and SOC pools, and the production of DOC is related to
221     these SOC and litter pools by empirical rate constants, which were fitted to reproduce observed DOC turnover
222     times (Kalbitz et al.,2003, Turgeon, 2008) and DOC concentrations in the soil. The much higher DOC
223     production rates simulated by ORCHIDEE-SOM in its original configuration during preliminary tests over
224     Europe led us to implement the new approach (equations 4-7). While preserving the basic structure of
225     ORCHIDEE-SOM, we thus adapted the model in a way that organic C exchange occurs mainly among the
226     particulate litter and SOC pools, similar to the original Century model, while preserving the basic structure of
227     ORCHIDEE-SOM. The production of DOC is represented as a side product of this C exchange between pools of
228     litter and SOC, with production rates as used in ECOSSE. In the modified soil carbon module, we used the
229     parameter ω (Eqs. 4-7) as a scaling factor that determines how much DOC is produced by the decomposition of
230     litter and SOC. This parameter was calculated after Smith et al. (2010) as the ratio of production of DOC from
231     litter ($p_{DOC_L}$) and the SOC pools ($p_{DOC_{SOC}}$) to the decomposition rates of litter ($k_L$) and SOC ($k_{SOC}$). The initial
232     values for ω were 0.5 % and 3 % for the litter and SOC pools, respectively. Further optimization with regard to
233     reproducing observed soil DOC concentrations led to ω values set at 0.2% for the litter and 1.2% for the SOC
234     pools.
235     Once produced, the free DOC can then be adsorbed to soil mineral particles, and the adsorbed DOC can again be
236     desorbed and return to the free DOC pool following a linear adsorption isotherm as described in Neff and Asner
237     (2001) and Wu et al. (2014). We assume that equilibrium between the dissolved and absorbed phases is
238     instantaneous. Moreover, the work by Kothawala et al. (2008) showed that this approach performed fairly well
239     compared to the more complex approach of using Langmuir equations. The partitioning is controlled by $K_D$, the
240     so-called equilibrium partition coefficient (eq. 9), considered constant at $8.05 \times 10^{-5}$ m³ water kg$^{-1}$ soil (Moor et
241     al., 1992). All constants used are listed in table S1.
242

$$DOC_{adsorption-desorption\,eq} = K_D * DOC \qquad\qquad (9)$$

243     Finally, the DOC pool is subject to decomposition according to equation (10) and then partly feeds into the SOC
244     pools (eq. 11), where $k_{DOC}$ is the DOC decay rate, which also depends on soil moisture and soil temperature.
245

$$CO_2\ respiration(DOC) = (1 - CUE) * k_{DOC} * DOC \qquad\qquad (10)$$
$$SOC\ production\ by\ DOC = CUE * k_{DOC} * DOC \qquad\qquad (11)$$

246     **2.1.3 Manure as an additional C source**
247     In Europe, a large fraction of the landscape is dominated by agricultural and grazing activities, and manure
248     application represents a significant additional C - in particular DOC- source to the soil in regions dominated by
249     grasslands and croplands. Studies have shown an increase in riverine DOC concentration related to manure
250     application, with frequency and intensity of storm events in spring directly after manure application exerting an

important control on the amounts of additional DOC leached to the river network (e.g., Royer et al., 2007; Delpla et al., 2011; Singh et al., 2014; Humbert et al., 2020). The type of manure input can be very different from one region to another, and the physicochemical properties (e.g. C:N ratio and the ratio of dissolved and particulate organic matter) depend strongly on the specific type of manure input. However, current forcing data only provide the amount of total manure inputs, without information regarding specific composition and/or physicochemical properties of the manure. To constrain the C flux from manure infiltrating into the soil, we used the gridded estimates of manure nitrogen (manure-N) applications produced by Zhang et al. (2017) as forcing file. Following the use of that data as forcing in the model branch ORCHIDEE-CNP developed by Sun et al. (2021), we assumed that 90% of the total manure-N is in mineral form (i.e. $NH_4^+$ or $NO_3^-$) and the remaining 10% is in organic form. To convert the organic manure-N into a manure-C flux, a C:N stochiometric ratio of 13.7 was then applied (Vuichard et al., 2018). Finally, the particulate and dissolved organic manure-C were assumed to feed the litter and DOC pools, respectively (Fig. S1). Consistent with ORCHIDEE-CNP (Goll et al., 2017), the fractions of particulate and dissolved manure-C were set to 0.9 and 0.1, respectively.

### 2.1.4 Hydrological processes

The representation of hydrological processes is handled in two distinct sub-modules. The first one, the hydrology sub-module, simulates the vertical exchange of water in the atmosphere-vegetation-soil system in each model grid cell, while the second one, the river routing module, simulates the horizontal transfers between grid cells. The hydrology is forced by several meteorological fields such as precipitation and air temperature. In the hydrology module, precipitation is divided into interception and throughfall, the latter being further subdivided into surface runoff and infiltration into the soil. The infiltration rate is controlled by the throughfall rate, the slope of the soil surface and the hydraulic conductivity of the soil which is a limiting factor for infiltration. The distribution of water within the soil is represented by the distribution of soil moisture over the discretized soil profile (de Rosnay et al., 2002, d'Orgeval et al., 2008). The water budget within the soil is thus determined by the infiltration rate and runoff from the top soil, the evaporation and transpiration from the soil, and drainage at the bottom of the soil column. The infiltration rate and percolation through the soil profile are used to compute the advective flux of DOC (equation 2)

The second module deals with river routing and represents the horizontal transfers of water from the soil column to the aquatic system though surface runoff and drainage, and further through the river network and adjacent floodplains (Vorosmarty et al., 2000). Meybeck (1993a,b) found that soils were the major source of DOC to rivers, while autochthonous DOC being negligible at the global scale. Furthermore, autochthonous DOC has a short turnover time and is quickly recycled within the river (Farjalla et al., 2009; Fonte et al., 2013) and, therefore, does not contribute significantly to the net C budget of an entire river system. Since in this study the focus is on the role of fluvial DOC fluxes in the terrestrial C budget, autochthonous DOC is not accounted for. The representation of leaching processes in ORCHILEAK is simplified, the model represents flows of water from land to the stream network only through surface runoff and drainage from bottom soil. Leaching thus occurs either from the topsoil, which in our configuration represents the top 4.5 cm of the soil column, or from

the bottom soil, i.e. the lowest 50 cm of the 2 m soil profile. DOC leaching from the top soil is further limited by two reduction factors, a 'general reduction factor' and a 'reduction factor for export with runoff depending on extends of saturated soils around headwaters'. The general reduction factor accounts for the fact that some of the runoff represents excess throughfall that never entered the soil and further corrects for the overestimated DOC concentration in the topsoil. The second reduction factor represents the connectivity between streams and their catchment through the extent of the water saturated riparian zone at sub-grid level, which varies with the amount of runoff and water stored in the "slow reservoir" of water, mimicking the groundwater storage. Note that for larger river stretches (stream order 4 and higher), ORCHILEAK simulates the occasional inundation of the river's floodplains, where DOC production from decomposition of litter and SOC in the top-soil, although being reduced under inundated conditions, feed directly into the DOC pool of the water column. For a detailed description of these features, please refer to Lauerwald et al. (2017).

**2.2 Simulations**

**2.2.1 Model set-up**

**Model domain, land cover and forcing data.** The simulated model domain extends over the area ($4.1 \times 10^6$ $km^2$) between 35°N and 70°N latitude and 10°W and 30°E longitude (Fig. 2). This domain includes 5600 model grid cells at 0.5×0.5° resolution and encompasses 6 broad climate zones according to the Köppen-Geiger classification from Peel et al., 2017 (Fig. 2a). The dominant PFTs within Europe include croplands (20% mainly C3), grasslands (31%, of which 24% are C3), and forests (39%, of which 16% and 9% are needleleaved evergreen and broadleaved summer-green boreal forests, respectively, while temperate broadleaved summer-green, needleleaved and broadleaved evergreen forests take 8%, 3%, and 3%, respectively) (Fig.2b). The spatial distribution of manure application on grasslands and croplands is shown in Fig.2c. Finally, Fig.2d illustrates the actual river network derived from the HydroSHEDS DEM data (Lehner et al., 2008) and the one corresponding to our river routing scheme at 0.5 degree resolution, highlighting that the representation of the river network is not optimal due to the coarse spatial resolution of our model. This coarse resolution limits the possibility of model validation to the downstream parts of larger river networks. Note further that the mouth of the Rhine is more than 100 km too far east, which further limits model validation for that river.
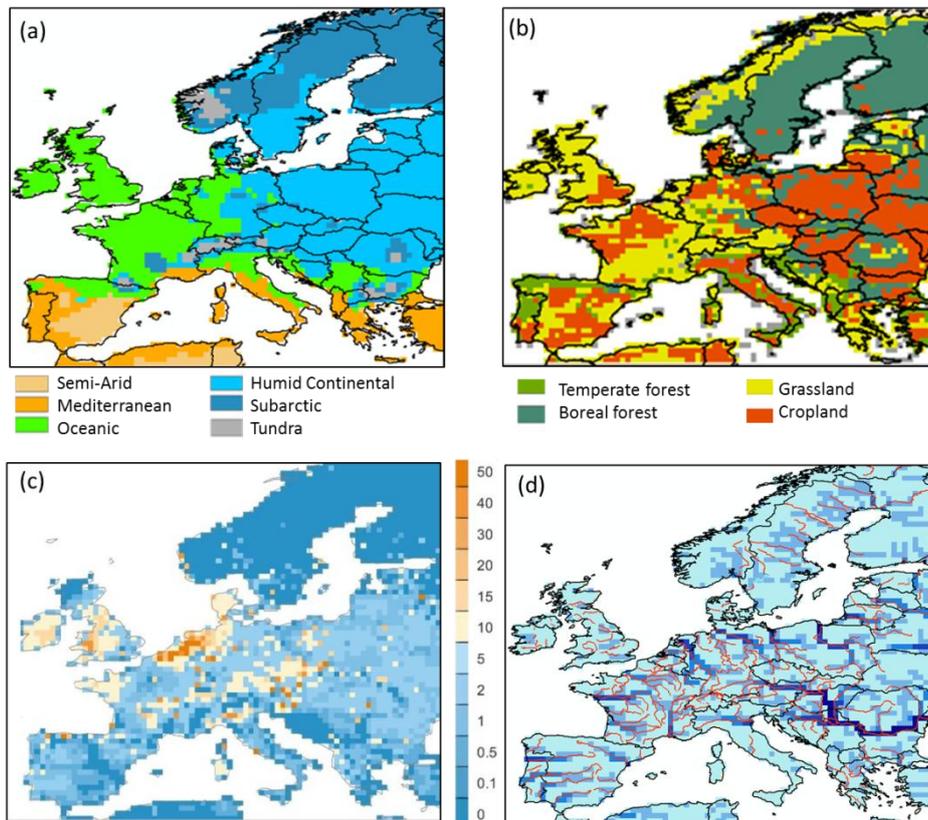
Figure 2. Spatial distribution for each 0.5° grid cell of the continental European domain of (a) climate zones (according to the Koppen-Geiger classification); (b) dominant plant functional types (PFT) (c) manure application (in gC m⁻² yr⁻¹); (d) the routing Network of ORCHILEAK (in blue). The real river network extracted from the European Environment Agency (https://www.eea.europa.eu/legal/copyright) is also shown.

The forcing data applied in our study are listed in table 1. They are the same as those used in Lauerwald et al. (2017) except for the meteorological forcing data and the land cover. The WFDEI meteorological forcing dataset used in this study was derived by applying the methodology originally used to create the WATCH Forcing Data (WFD) from the ERA-Interim reanalysis data (Weedon et al., 2014). The dataset has a 0.5° spatial resolution and a 3-hourly time step from 1978 to 2014. The land cover forcing data set, which gives the areal proportion of the 13 PFTs within each 0.5° grid cell, was taken from Peng et al. (2017). Note that the soil hydrology model in ORCHIDEE, which we adopted for ORCHILEAK, was developed and calibrated to work with the soil classes used in Reynolds et al. (1999). We thus kept that data source, while additional soil properties such as pH and specific soil classes which we defined as "poor soils" (Histosols, Podzols) with lower C turnover times and DOC filtering were taken from HWSD v1.1. A topographic index, which in ORCHIDEE controls the flow velocity in the river network of each cell is taken from Vorosmarty et al. (2000). "Floodplains", defined as the maximum areal proportion of a grid cell that can be flooded when the river exceeds its bankfull flow, and "Swamps" representing groundwater fed wetlands in the floodplain, were adopted from the Global Lake and Wetland database (Lehner and Doll, 2004). Depending on the areal extend of these swamps, a proportion of stream flow

334 is simulated to feed into the soil moisture storage of the grid cell considered. Both parameters have an effect on
335 the simulated river discharge and soil hydrology in the floodplains. For details, see Lauerwald et al. (2017).
336

337 **Table 1. List of the forcing files used for our simulations, along with their spatiotemporal resolution.**

| VARIABLE | SPATIAL RESOLUTION | TEMPORAL RESOLUTION | DATA SOURCE |
|---|---|---|---|
| Rainfall, snowfall, incoming shortwave and longwave radiation, air temperature, relative humidity and air pressure, wind speed. | 0.5° | 3 hours | WFDEI_GPCC (WATCH Forcing Data (WFD) by making use of the ERA-Interim reanalysis data, Global Precipitation Climatology Centre; Weedon et al. (2014)) |
| Soil texture class | 0.5° | - | Reynolds et al., 1999 |
| Soil pH, soil bulk density, poor soil | 0.5° | - | HSWD v 1.1 (Fao et al., 2009) |
| Stream flow directions and topographic index | 0.5° | - | STN-30p (Vörösmarty et al., 2000) |
| Floodplains and swamps | 0.5° | - | Guimberteau et al., 2012 |
| River surface area | 0.5° | - | Lauerwald et al., 2015 |
| 10th, 50th, 90th percentile of the stream reservoir | 1° | - | Derived from pre-runs with ORCHIDEE |
| Land cover | 0.5° | - | Peng et al. (2017) |

338

339 **Parametrization of hydrological processes**. ORCHILEAK was previously parametrized and validated for the
340 Amazon (Lauerwald et al., 2017; Hastie et al., 2019; Lauerwald et al., 2020), Congo (Hastie et al., 2021) and
341 Lena (Bowring et al., 2020) basins. In our study of the European river network, we updated ORCHILEAK with
342 the more recent hydrology scheme of the recent standard version of ORCHIDEE (svn 5091). This hydrology
343 scheme has been calibrated against observed runoff at a global scale (Ringeval et al., 2012; Yang et al., 2015).
344 Furthermore, MacBean et al. (2020) has evaluated the model performance for simulating soil moisture in
345 temperate ecosystem. This new hydrology scheme features a dynamic surface roughness of the vegetation, which
346 decreases the aerodynamic resistance near the surface when vegetation cover is low, leading to lower ground
347 temperatures and thus lower evaporation rates. This adjustment was deemed necessary in order to better capture
348 the observed mean and seasonal variability of the discharge along the European river network. The two reduction
349 factors controlling DOC leaching from the top soil to the headwaters streams were also adjusted (see 2.1.4).

350 **Spin-up.** Before the model can be used to simulate C dynamics over the past decades, a spin up is needed to
351 reach an assumed steady state for the C fluxes during the pre-industrial period. This steady state is achieved by
352 spinning up ORCHILEAK for 15000 years. The spin up was realized by recursively looping over 4 years of
353 climate forcing using the WFDEI forcing dataset over the 1979-1982 period (because the first year of the
354 forcing, 1978, is incomplete) and constant land cover and atmospheric $CO_2$ concentration of 286 ppm
355 (Guimberteau et al., 2018) corresponding to year 1861. After the end of the spin-up, the soil C stock across the
356 entire European continent changed by less than 1% over a century of simulation, which we considered close
357 enough to steady-state.

358 **Transient runs.** Using the steady-state outputs as initial condition, the first part of the transient simulation
359 (1861-1978) was carried out with increasing atmospheric $CO_2$ concentration, changing land use and land cover
360 and with river routing activated while still looping over 27 years (1979-2006) of the WFEDI forcing dataset.
361 From 1979 onwards, the WFDEI atmospheric forcing data was applied over the entire period covered by this
362 product with the changing land cover map and atmospheric $CO_2$ values applied for each year of simulation.

363

364 **2.2.2 Model evaluation**

365 Firstly, the simulated discharges were compared to times series of daily stream flow recorded at eleven gauging
366 stations from "The Global Runoff Data Center (GRDC), 56068 Koblenz, Germany" dataset. For comparison,
367 both observed and simulated discharges were aggregated at the monthly temporal resolution over the years 1980
368 to 2006. Note that the river network in ORCHILEAK does not always match the real river network. The selected
369 gauging stations were assigned to the cell best representing the parts of the river network to which the sampling
370 location corresponds. However, important correction had to be performed for the most upstream stations in the
371 Rhine and the Elbe river network. The period 1980 to 2006 was chosen based on the GRDC data coverage.

372 Model performance was further evaluated with respect to several variables of the terrestrial C cycle. Firstly,
373 simulated Net Primary Production (NPP) was compared to two different data products. The first one, the
374 CARbon DAta MOdel fraMework (CARDAMOM; Bloom et al., 2015) built from model data fusion analysis at
375 1° resolution. The second one is the Global Inventory Modeling and Mapping Studies (GIMMS) at 0.5°
376 resolution based on AVHRR and MODIS sensors. GIMMS uses several atmospheric forcing data set to derive
377 NPP. Those are CRUNCEP version 4 P1 and P2 (Rainfall, cloudiness, relative humidity and temperature taken
378 from the CRU (Climate Research Unit), while the other fields such as air pressure, longwave radiation, wind
379 speed are directly derived from NCEP (National Center for Atmospheric Research)), ECMWF (European Centre
380 for Medium-Range Weather Forecasts), MERRA2 (the Modern-Era Retrospective analysis for Research and
381 Applications, Version 2) and NCEPR2 (https://www.esrl.noaa.gov/psd/). For our comparison, we calculated the
382 average of the NPP obtained with these five atmospheric forcing files. The NPP values from ORCHILEAK and
383 GIMMS were averaged over the period 1982-2006 while CARDAMOM only covers a shorter time period
384 comprised between 2001 and 2010. Modelled NPP was then compared to the NPP data products at the European
385 scale and at the scale of five large European basins for which we also evaluated the simulated river discharge and
386 DOC fluxes, and which taken together, represent 19 % of the model domain (Fig.3): the Danube, Rhine, Elbe,

387     Rhone and Seine. All five basins are located in an oceanic or humid continental climate (Fig.2a) although the

388     Rhone basin extends further into the Mediterranean climate zone. The basin characteristics according to land

389     cover types are as follows: the Danube and the Elbe basins have both a high proportion of croplands (around

390     40%), the remainder being mostly covered by grasslands and boreal forests. The Rhone is covered by 50% of

391     grasslands, while in the Seine basin croplands reach 50%. The Rhine has a more diverse land cover with a

392     substantial proportion (about 30%) of boreal (10 %) and temperate (20 %) forests, 35% of grasslands and 25% of

393     croplands. See table S2 for further details.
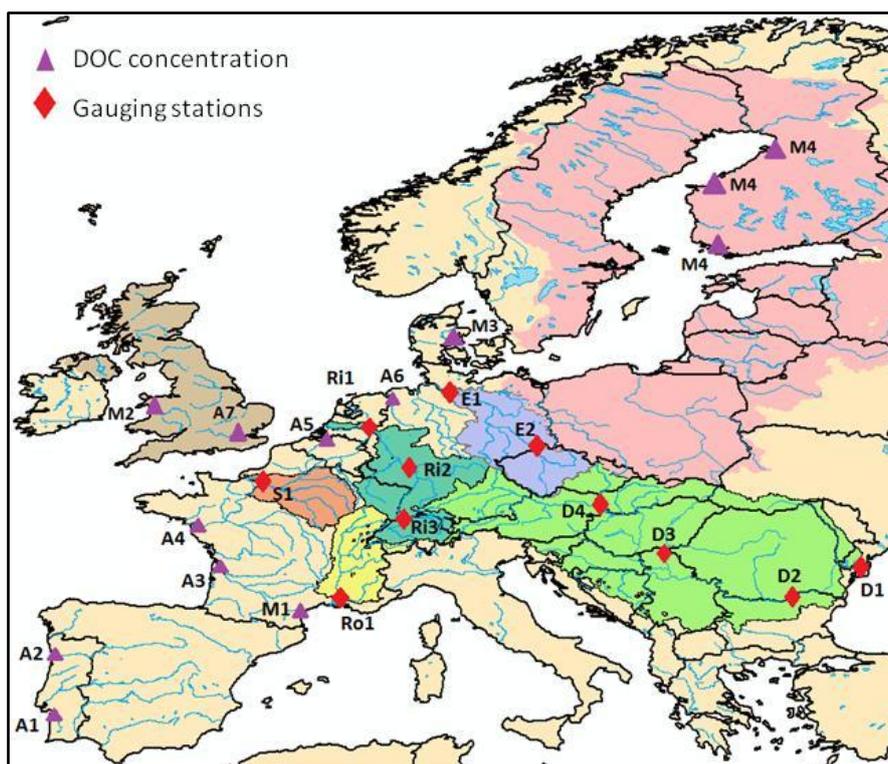
394

395 **Figure 3. Map of continental Europe delineating the (group of) catchments of focus in this study and the location of**
396 **observed discharge and DOC concentrations. Catchments, from west to east are: All UK (light brown), Seine**
397 **(orange), Rhone (yellow), Rhine (dark green), Elbe (violet), All Baltic (pink) and Danube (light green). Observations**
398 **include GRDC stations (red diamonds) in the Seine (S1-Poses), Rhone (Ro1-Beaucaire), Rhine (Ri1-Lobith, Ri2-Main**
399 **in Frankfurt, Ri3-Basel), and Danube (D1-Ceatal Izmael, D2-Svistov, D3-Tisza in Senta, D4-Bratislava) catchments,**
400 **as well as river stations where DOC concentrations were measured (purple triangles): A1-Douro, A2-Sado, A3-**
401 **Gironde, A4-Loire, A5-Scheldt, A6-Ems, A7- Wales, A8-Thames, M1-Tech, M2-Wales, M3-Denmark, M4-Finland**
402 **(Abril et al 2002, Mattsson et al., 2008).**

403

404     The soil temperature is compared to the soil temperature generated using data from the European Centre for

405     Medium-Range Weather Forecasts reanalysis ERA5 dataset (Munoz-Sabater et al., 2021). The soil heterotrophic

406     respiration (SHR) is compared against the data-driven global SHR dataset published by Yao et al. (2020). The

407     global SHR data set was produced using a Random Forest algorithm, up-scaling from 455 data points from the

408     Global Soil Respiration Database (SRDB 4.0) based on gridded fields of climatic, edaphic and productivity

409     related variables as predictors (Yao et al., 2020). We compared the results of ORCHILEAK with the average,

minimum and maximum values of SHR estimated by Yao et al. (2020). SOC from the Harmonized World Soil Database (HWSD) was used to evaluate the simulated SOC stocks. HWSD is a global soil database that contains up-to-date information on a large range of soil properties. For instance, this dataset reports the organic carbon content in the soil as well as the soil bulk density. The bulk density in HWSD was calculated in two different ways. The first one follows the method described in Saxton (1986) where the bulk density is related to the soil texture - an approach tending to overestimate density in high porosity soils or in OC rich soils. The second method uses the SOTWIS database in which the bulk density is calculated as a function of soil type and depth. In this database, all variables are reported for the topsoil (0-30cm) and the sub-soil (30-100cm) horizons. For comparison purposes, our simulated SOC stocks were thus integrated over the same depth intervals. We further assessed the extent to which our model can reproduce the main features in observed soil DOC profiles. To that end, we compared our simulated DOC profile averaged over the entire European forest biome against the one established by Camino et al. (2014) on the basis of a synthesis of local measurements. Although there are many studies on DOC concentrations in the soil, we selected the one by Camino et al. (2014) because it provides a synthesis at the pan-European scale, and is thus ideal to extract "representative" concentration profiles over a sufficiently large domain, compatible to the regional scope of our study. Unfortunately, similar synthetic profiles based on observations have not been constructed for croplands and grasslands.

The key variables of interest in our study are the DOC leaching flux from the soil and the DOC export flux to the coast. These fluxes require accurate simulation of the water discharge fed by runoff and drainage as well as of DOC concentrations in the leaching flux and in the riverine flux. For the leaching flux, our simulation results were compared to measured fluxes reported by Kindler et al. (2011) across different locations in Europe. Because the observed DOC leaching fluxes from both top and bottom soil reported by Kindler et al. (2011) are based on local measurements that are not easily comparable to simulated fluxes at the coarse spatial resolution of our model (0.5° or about $2*10^3$ km² at the corresponding latitude), we consider the comparison against measured river DOC fluxes more relevant for our purpose, as rivers are good integrators of mean, larger-scale catchment properties. For the riverine export fluxes, we assessed the modeled discharges and DOC concentrations separately. For evaluation of stream DOC concentrations, DOC data were extracted from the GLObal RIver CHemistry database (GLORICH, Hartmann et al., 2014) for the Rhine and Elbe basins and from the "Eau de France" database for the Seine and Rhone basins. These data were complemented by river DOC concentrations reported by Abril et al. (2002) for 9 river mouths (Sado, Thames, Ems, Scheldt, Gironde, Douro, Loire, Elbe and Rhine), and by Mattsson et al. (2008) for several river basins located in Finland, Denmark, Wales and France.

**3 Results and discussion**

**3.1 Model evaluation at pan-European and catchment scales**

**3.1.1 Discharge**

Figure 4 compares the simulated discharge against observations for selected stream gauging stations (section 2). Those stations are located near the mouth of large rivers (Danube, Rhine, Rhone, Elbe and Seine) but also include a few locations further upstream the same rivers or at major tributaries (Fig.3). The comparison is

446  performed for the period 1990-2000, except for the Rhone at Beaucaire and the Danube at Svistov for which the
447  observed stream gauge data cover only a shorter period. Overall, the model reproduces the observations well,
448  both in terms of amplitude and seasonality, except for the Elbe at Neu Darchau, for which the temporal
449  variability is well captured but the absolute discharge is overestimated.

450  Note that the simulated catchment area often diverges (by -25% to +30 %) from the observed value due to the
451  coarse resolution (0.5°x0.5°) of ORCHILEAK (Table S3). As a result of the model resolution, smaller tributaries
452  are not represented individually and each grid cell was fully assigned to one larger river basin. The effect of the
453  resolution is also shown in Fig.2d which compares the observed and modeled river network. Discrepancies
454  between model and real world catchment area will translate into proportional biases in discharge simulation.
455  Furthermore the 0.5° resolution is too coarse to be able to represent perfectly the pathways of the river. Our
456  model tends more often to underestimate the catchment area, while its yearly mean discharge is overestimated,
457  except at the Beaucaire station along the Rhone River.  The bias can be significant and cannot be explained by
458  the model resolution alone.
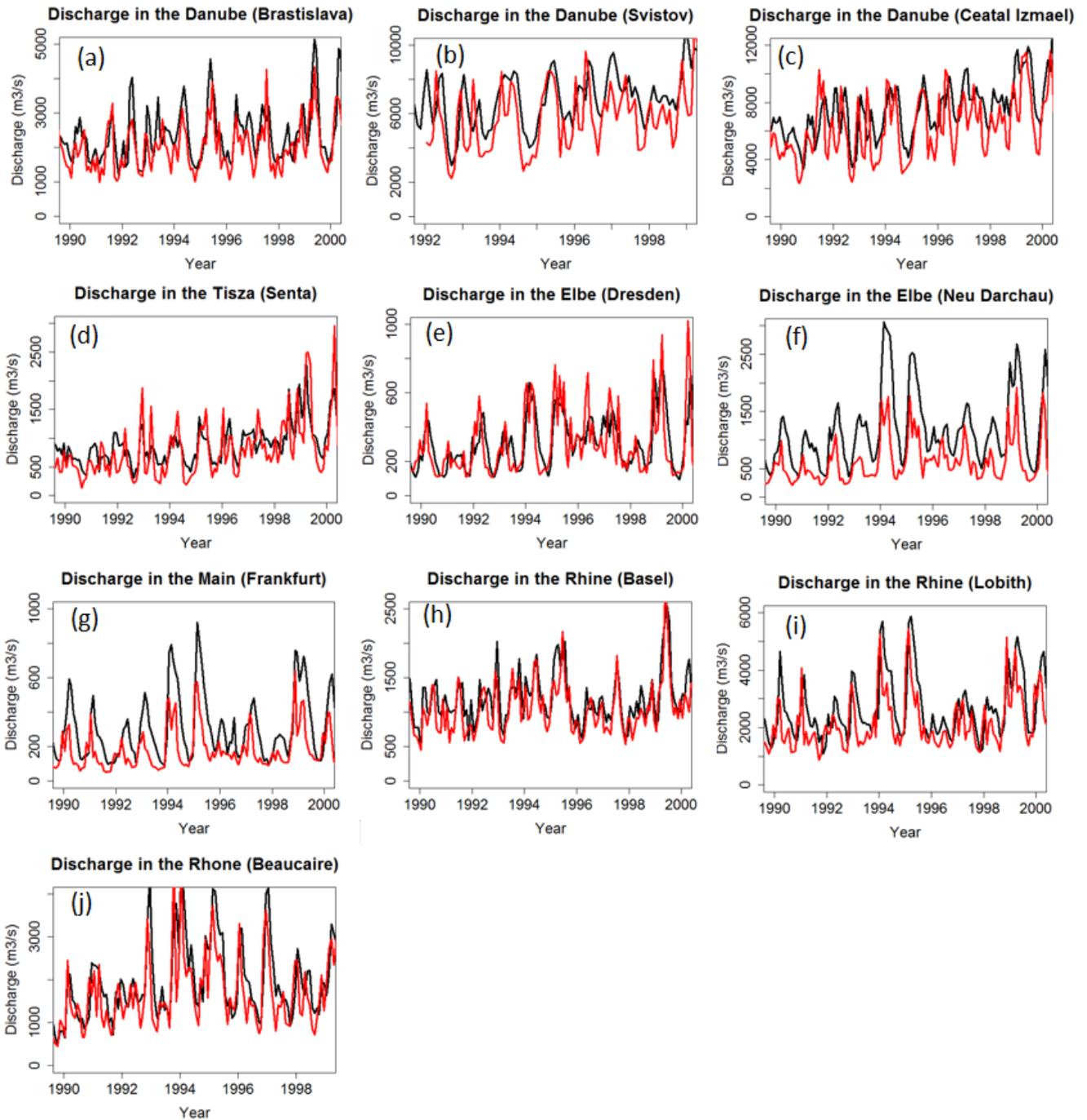
**Figure 4. Modeled (black) and observed (red) time series of discharge at the GRDC gauging stations in the Danube (a-c) and its tributaries (d), Elbe (e-f), Rhine and its tributaries (g-i) and Rhone (j). Note the different time periods of measurements. See Figure 3 for exact location.**

To evaluate model performance for discharge, we used the Pearson's coefficient of determination ($R^2$) and the Nash Sutcliffe modeling efficiency (NSE, Nash and Sutcliffe (1970)). The $R^2$ only accounts for the correlation with regard to the temporal variability. With $R^2$ values comprised between 0.43 and 0.62 for all stations, we conclude that the observed seasonality of the discharge along large European rivers is reasonably well reproduced by the model. The NSE not only accounts for the correlation between observed and simulated temporal signals, but also for the model's ability to reproduce absolute discharges. The statistics confirm our previous observation that the model generally overestimates discharges (low NSEs) except for stations Elbe in Dresden, Rhone in Beaucaire, Rhine in Basel and Danube in Bratislava where both the mean and temporality are well captured. Two stations have negative NSE values, which means that the error variance estimated by the model is significantly larger than the variance of the observations; in others words, the difference between model and

observations is significant. The mean error (%), that is, the weighted difference between the average from the model and the one from observation, confirms that low NSEs are mostly due to overestimated discharges, which is further demonstrated by high mean errors. More results for other European catchments can be found in table S3.

### 3.1.2 NPP, SHR, soil temperature, biomass and soil organic C stocks

We briefly compare simulated NPP with the gridded observation-based products GIMMS and CARDAMON (section 2.2.2) as C fixation by the vegetation exerts an important control on DOC stocks in the soil and thus on DOC leaching. We first perform our comparison over a large domain comprised between -10° and 30° in longitude east and 35° and 70° in latitude north - covering the area from Ireland to the Western Black Sea (where the Danube flows into) and from the south of Spain to the north of Scandinavia. Over this area (referred to as "Europe" from here onwards), the modeled yearly averaged NPP amounts to 445 gC m$^{-2}$ yr$^{-1}$, a value in remarkable agreement with both GIMMS and CARDAMOM estimates of 430 gC m$^{-2}$ yr$^{-1}$ and 460 gC m$^{-2}$ yr$^{-1}$, respectively. Those two datasets are entailed with an uncertainty that we assume similar to that reported for the MODIS dataset, i.e. 20% (Turner et al 2006). The total living biomass in Europe is simulated at 15.5 PgC or 2.3 kgC m$^{-2}$. This value is in good agreement with the recent estimate by Avitabile and Camia 2018, which report a biomass stock at around 16 PgC. We estimate that the total soil carbon stock amounts to 58 PgC. Averaged over the first meter of the soil horizon, this corresponds to a value of 9.5 kgC m$^{-2}$ which is comparable to that of HWSD (6 kgC m$^{-2}$) when using the SOTWIS method to compute the bulk density, but significantly lower when applying Saxton's method (22 kgC m$^{-2}$), plausibly because the latter overestimates the bulk density in OC-rich soils (Kochy et al., 2015). Results at the catchment scale are described in the supplementary section.

Figure 5a shows the comparison of simulated vs. data driven estimates of soil temperature. Soil temperature is overall well represented with a simulated mean temperature of 8.4° C against 9.3°C after ERA5. The overall slight underestimation is due to a substantial underestimation of soil temperatures in the northern regions. Furthermore, this underestimation is more important in the winter (January, February and March) with a difference relative to ERA5 values reaching 3.5°C, while in summer (July, August and September) this difference amounts to only 0.5°C. This underestimation is due to the poor representation of the isolating effect of the snow cover in ORCHIDEE (Wang et al., 2013).

The comparison of simulated SHR against Yao et al.'s estimate is shown in Figure 5b. Over Europe, ORCHILEAK underestimates the SHR compared to Yao et al.'s estimates by about 14%, with a simulated average of 312 gC m$^{-2}$ yr$^{-1}$ against an average of 363 gC m$^{-2}$ yr$^{-1}$ (range from 317 to 417 gC m$^{-2}$ yr$^{-1}$) estimated by Yao et al. (2020) for the period 1985-2013. Looking at specific climatic regions, some regions are well represented in ORCHILEAK, as the Mediterranean and humid continental regions with a mean SHR of 371 and 363 gC m$^{-2}$ yr$^{-1}$, against 385 and 354 gC m$^{-2}$ yr$^{-1}$ from Yao et al., respectively. SHR in semi-arid and tundra regions are on the contrary around 50% lower than Yao et al.'s estimate. For the tundra region the underestimation in SHR is consistent with an underestimation of the NPP (see table S4).
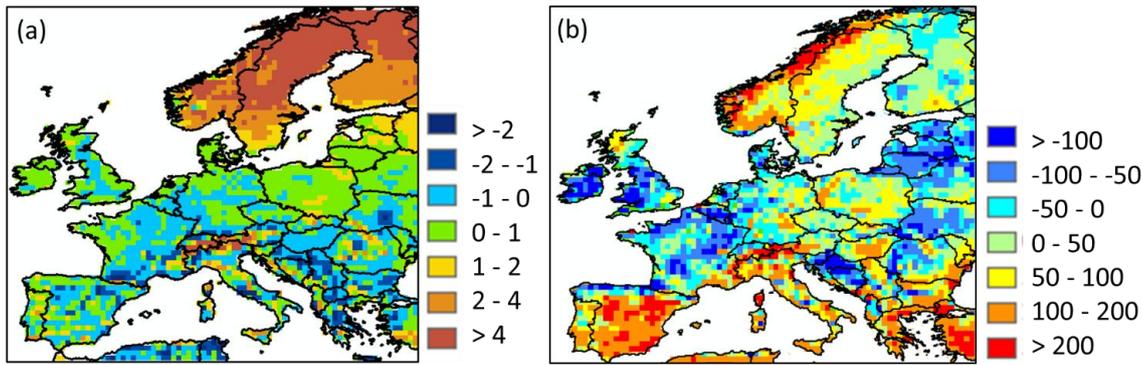
**Figure 5. Difference in (a) simulated soil temperature (in °C) against values reported by ERA5; (b) simulated soil heterotrophic respiration (in gC m⁻² yr⁻¹) against values reported by Yao et al. (2020).**

### 3.1.3 Soil DOC stocks

Comparison between observed and modeled DOC stocks and fluxes is more difficult than for biomass and SOC because those have not been assessed at large spatial scales. Nevertheless, representative soil DOC concentration profiles for coniferous and broadleaved forests of Europe have been compiled by Camino et al. (2014). These profiles were used to evaluate our model. Overall, we found that ORCHILEAK slightly overestimates DOC concentrations, especially in the very topsoil layers with modeled values of around 100 mg l⁻¹ against 40-60 mg l⁻¹ in the observations (Fig. 6). We also simulated higher concentrations in broadleaved forests than in coniferous forests while Camino et al. (2014) obtained the opposite. When integrated over the first meter of the soil horizon of forested ecosystems (28 % of the European land area), the modeled and observed DOC stocks amount to 22.2 and 11.3 gC m⁻², respectively. Above, we have shown that over Europe SOC stocks were underestimated while the average DOC concentrations in the soil over all European forests are here overestimated. One explanation for the underestimation of SOC stocks and the likely overestimation of DOC stocks is thus that SOC decomposition rates in the new soil carbon module may be slightly too high. It is however difficult to generalize this conclusion because of the lack of synthesis data for other land cover types, especially croplands and grasslands which together represent about 50 % of the total European land area. Modeled DOC stocks averaged over broad climate regions reveal highest values for the oceanic climate with 32 gC m⁻² and the Mediterranean climate with 26 gC m⁻². Semi-arid and humid continental climates have similar stock densities of respectively 17.5 and 20 gC m⁻² and it is in the coldest climates (subarctic and tundra) that we find the lowest DOC stock densities of around 8 gC m⁻².
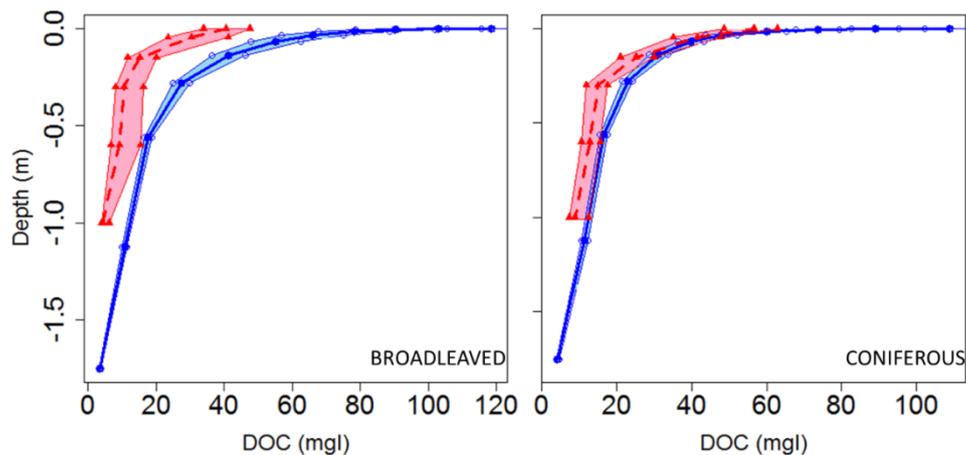
**Figure 6. Modelled (blue) versus observed (red dashed) DOC concentration profiles averaged over the soils of the European Coniferous and Broadleaved forest biome. Data from Camino et al. (2014). The shaded area represents the 95% bootstrap confidence interval for model and observations.**

**3.1.4 DOC leaching fluxes**

The model simulates a yearly-mean DOC leaching flux over Europe of 14.3 (±10) TgC yr$^{-1}$ (Fig 7), the standard deviation

535   being here coarsely approximated by spatial variability. The average area specific flux rates amounts to 2.6 (±2.5) gC m$^{-2}$ yr$^{-1}$. We compared DOC leaching fluxes with site level observations from Kindler et al. (2011), across 17 local measurements, each sampled fortnightly during the period October 2006 until March 2008. Comparing model results at 0.5° resolution to point measurement is complicated, and thus in this section, we compare only our model-averaged result against the 17-site average from Kindler et al. (2011). Our modeled average of 2.6 (±2.5) gC m$^{-2}$ yr$^{-1}$ is of the same order of magnitude as the

540   observed one (4.2 gC m$^{-2}$ yr$^{-1}$). Although the modeled mean is about 38 % lower than the one measured, the standard deviation representing the spatial variability in simulated DOC leaching fluxes over all our model grid cells encapsulate the observational mean, highlighting a significant heterogeneity that is difficult to embrace with local measurements alone. This comparison must be taken cautiously because of the limited number of observations and the resolution of our model. Furthermore, DOC leaching flux at the coast is generally not well represented. The reason is that DOC leaching fluxes are

545   normalized by the area of the whole cell. The area normalized flux at the coast is thus often lower.
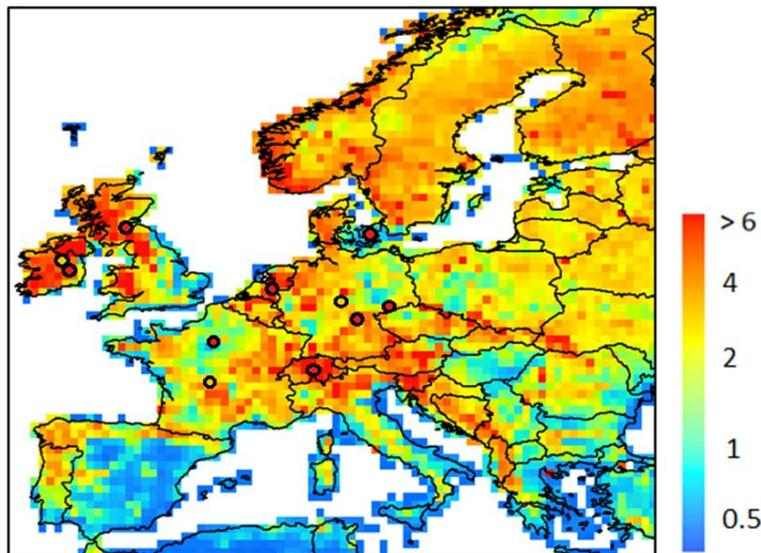
**Figure 7. Modelled yearly mean terrestrial DOC leaching flux (period 1979-2006) to the river European river network (in gC m$^{-2}$ yr$^{-1}$). The local observations from Kindler et al., 2010 are also reported, using the same scale. Note that the local observations cover a much shorter time period and may not be representative of the whole year.**

550

The seasonal distribution of the DOC leaching flux is shown in Fig. 8. On average, the leaching flux per season averaged over Europe amounts to 1.6, 1.3, 0.5 and 1.4 TgC month$^{-1}$ in winter, spring, summer and autumn, respectively. If we exclude the high latitude and high altitude regions (Scandinavia, the Alps), a clear seasonality is observed with the lowest fluxes in summer and spring and the highest fluxes in winter and autumn. In the high latitude/altitude regions, the pattern is different

555   with highest fluxes in spring which extends to the summer in the Alps, and corresponds to the snowmelt period. The highest fluxes per unit area are simulated in Scandinavia during the spring season, even though peatlands are not represented in the model. Some regions are leaching hotspots such as the Alps throughout the year, the West Balkans during autumn and the Western flank of the UK in autumn and winter.

gC/m².month

>0.5
0.25
0.1
0.05

0.01
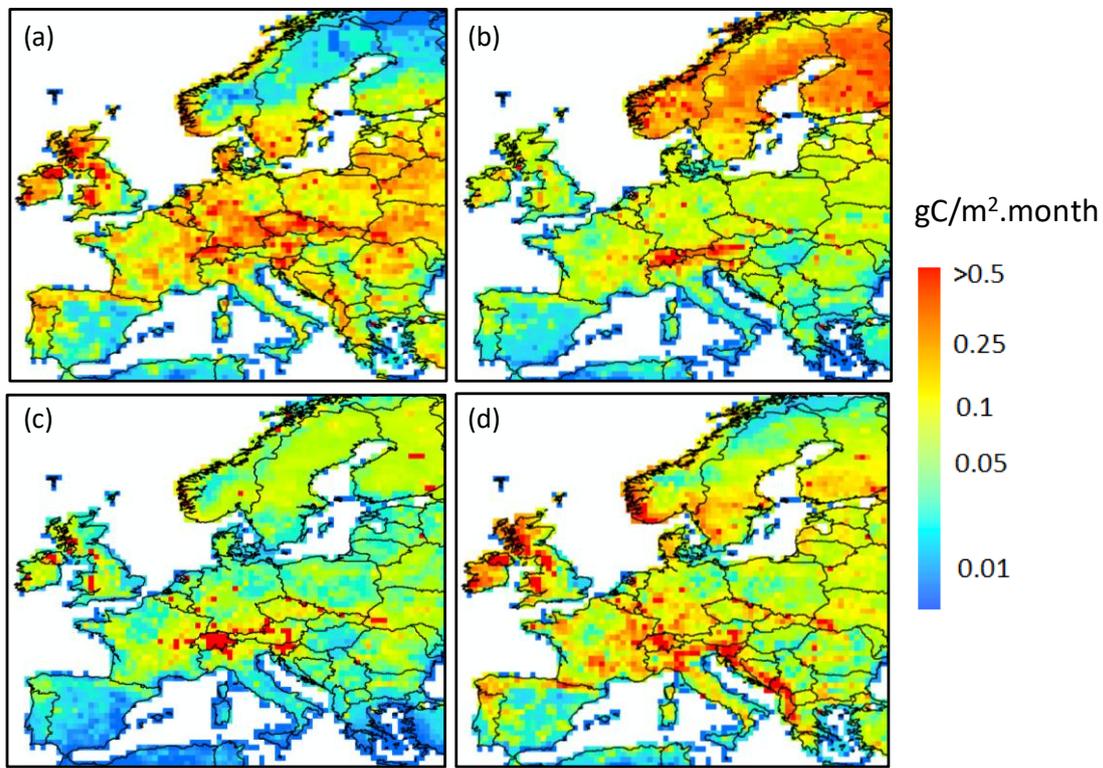
**Figure 8. Seasonal distribution of the terrestrial DOC leaching flux (gC m$^{-2}$ month$^{-1}$) for (a) Winter, (b) Spring, (c) Summer and (d) Autumn, averaged over the period 1979-2006. A logarithmic scale is used to better highlight the spatiotemporal gradients.**

### 3.1.5 Fluvial DOC decomposition and export fluxes

The export of DOC from the European river network to the coast is arguably the best monitored variable against which our model can be evaluated. Using this flux to build confidence in our estimate of the terrestrial DOC leaching requires an assessment of the DOC degradation within rivers, a process that is controlled by the hydrology and the half-lives of reactive DOC compounds. In the model, the first-order decomposition rates at a given temperature of 28°C are equal to 0.3 d$^{-1}$ and 0.01 d$^{-1}$ for the labile and refractory DOC pools, respectively. Based on those values and the simulated distribution of labile and refractory DOC, the estimated bulk decomposition rate constant averaged over the entire model domain is equal to 0.05 d$^{-1}$, which corresponds to a half-life for riverine DOC of about 14 days (Table 3). This rate constant varies across Europe but always remains within the same order of magnitude, with half-lifes ranging from 6 to 20 days (0.035-0.122 d$^{-1}$). These decomposition rates are in good agreement with the average rate reported by Berggren and Al-Kharusi (2020) of 0.037 d$^{-1}$ based on field experiments carried out at multiple river sampling locations across Europe. We thus conclude that DOC decomposition rates used in ORCHILEAK are reasonable, and fluvial DOC fluxes are a valid proxy to evaluate simulated DOC leaching fluxes.

**Table 3. Estimated river DOC decay rates applied in ORCHILEAK. Values are reported for four large river catchments and for the six dominant climate zones**

| REGIONS | | DECAY RATES (day⁻¹) |
|---|---|---|
| **BASIN** | Rhine | 0.074 |
| | Danube | 0.043 |
| | Meuse | 0.056 |
| | Rhône | 0.072 |
| **CLIMATE ZONE** | Semi-arid | 0.035 |
| | Mediterranean | 0.046 |
| | Oceanic | 0.053 |
| | Humid continental | 0.048 |
| | Subarctic | 0.064 |
| | Tundra | 0.122 |

580
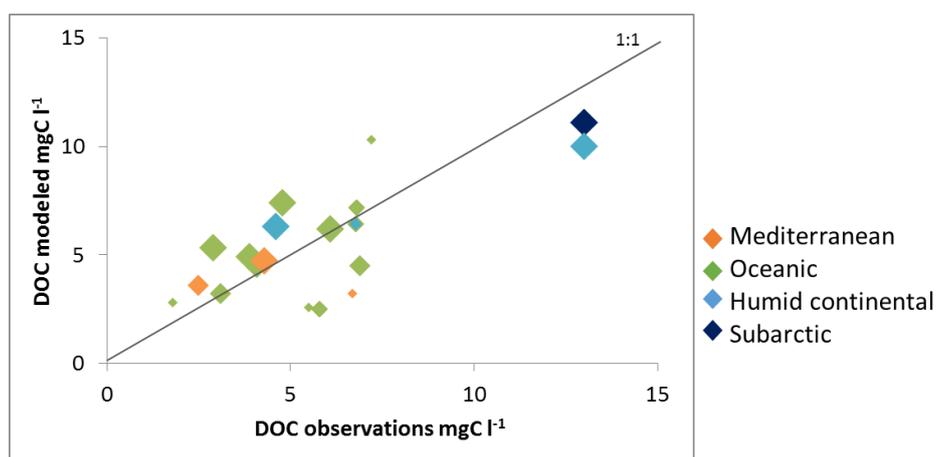
**Figure 9. Modelled river DOC concentration against observed values. The color code indicates the dominant climate zone for each catchment while the size of the diamond is proportional to the catchment area according to the following classes: < 10 000 km², < 50 000 km², < 100 000km² and > 100 000 km². See table S4 for further details.**

585     Figure 9 compares modeled versus observed multi-annual mean riverine DOC concentration at specific locations or within a group of small river catchments. Local DOC measurements include data near the mouth of the Rhine, Elbe, Rhône and Seine rivers (discharge, DOC concentration and fluxes for the Rhine and Seine in figure 10). In addition, Abril et al. (2002) report DOC concentrations measured at nine river mouths discharging along the Atlantic façade and the North Sea, three of which (Rhine (NL), Scheldt (BE) and Gironde (F)) resolve the seasonality while the other six (Elbe (GE), Ems (GE), Thames (UK),

590     Loire (FR), Sado (P), Douro (P)) only rely on a single measurement per year. Both GLORICH and Abril et al. (2002) report DOC concentrations at the mouth of the Rhine and the Elbe but their values diverge because in addition to analytical uncertainties, the sampling period and data density are not the same. Measured values are equal to 4.3 and 2.9 mg C l⁻¹ for the Rhine and 4.6 and 6.1 mg C l⁻¹ for the Elbe, respectively highlighting inherent variability in observational data. To complement these local samplings, we also compared our simulated DOC concentrations with those of Mattson et al. (2008)

595     for several groups of catchments in Finland (9 spread over the whole country), Denmark (10 draining into Horsens fjord), the UK (10 draining into the River Conwy) and France (5 draining into the River Tech). All measured DOC concentrations

ranged from 2.5 mg C l$^{-1}$ to 10 mg C l$^{-1}$ except in two regions in the north (Finland and basins flowing into the Baltic sea) where concentrations exceeded 10 mg C l$^{-1}$. For most of the data, the model slightly overestimated the river DOC concentrations. The model results also suggest that DOC concentrations broadly increase with latitude, with the higher
600 values found in humid continental and subarctic climate and the lower ones in the Mediterranean climate, a result in agreement with the observations from Mattson et al. (2008). Such pattern possibly results from decreasing mean annual air temperature and runoff in Northern Europe that favor incomplete decomposition of litter and soil DOC, thus favouring DOC production in the soil, while at the same time DOC turnover rates in the soils are decreased. Also the increased abundance of forests, and in particular coniferous forests, is a valid explanation for higher DOC leaching (Lauerwald et al. 2012).
605 However, it is important to keep in mind that we are not representing peatlands, suggesting that we could lack part of the DOC leaching in subarctic and tundra regions leading to even higher DOC fluxes further in the North. Finally, the comparison reveals that model performance tends to improve with catchment size, likely reflecting the difficulty to capture the DOC dynamics at the small scale with the current resolution of ORCHILEAK. But overall, our model is capable of reproducing observed yearly mean DOC concentrations for a wide range of river basins spread between Finland and
610 Portugal.
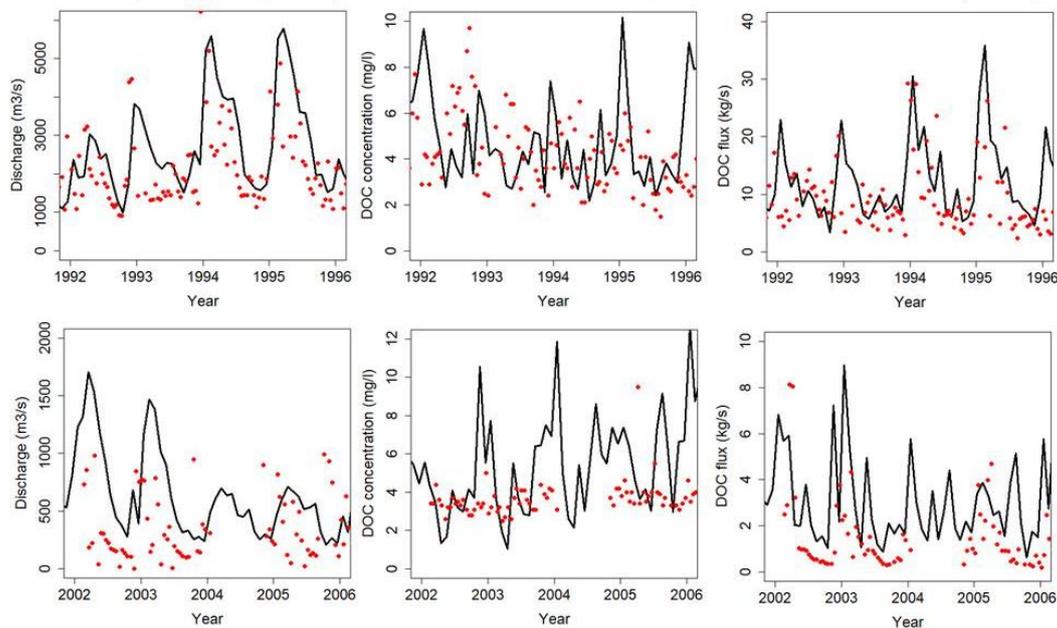
**Figure 10. Time series of discharge (left), DOC concentration (middle) and DOC fluxes (right) in the river Rhine at Lobith (top row, period 1992-96) and in the Seine at Poses (bottom row, period 2002-2006. See figure 3 for location of stations. (Black lines for**
615 **ORCHILEAK and red dots for observations)**

The temporal evolution of observed river DOC fluxes is only available at four stations (Rhine, Elbe, Rhône and Seine) where DOC time series have been recorded over multi-annual periods (Rhine and Seine illustrated in Fig. 10). In term of inter-annual variability (IAV), riverine DOC fluxes present the highest variability with a coefficient of variance (COV) of 0.62 for
620 the Seine and 0.57 for the Rhine. For comparison, IAV of discharge and riverine DOC concentration shows COVs of 0.60 and 0.51 for the Seine and 0.40 and 0.45 for the Rhine, respectively. The higher IAV for the flux is due to a tendency of higher concentrations coinciding with higher discharge, which is due to the flushing effect where higher discharges follow higher amounts of runoff from top-soils rich in DOC. The multi-year mean modelled DOC fluxes are estimated for the Rhine, Elbe, Rhone and Seine at 11.9, 7.2, 8.8 and 3.2 kg s$^{-1}$, respectively. The observations amount respectively to 7.9, 3.6,
625 4.6, 1.6 kg s$^{-1}$. For all stations, the model thus slightly overestimates fluvial DOC fluxes, which is not surprising since the model tends to overestimate the discharge. At these four stations, ORCHILEAK also slightly overestimates river DOC

concentrations except for the Seine where concentrations are largely underestimated and discharge largely overestimated. In terms of temporal correlation, the simulated DOC flux for the Rhone compared to the observed one yields a $R^2$ of 0.6 and a mean error of 92% (results for the Seine, Elbe and Rhine are reported in supplementary table S6). In figure 9, we clearly see a large overestimation of the temporal variability in DOC concentrations and this could lead to an overestimation in DOC fluxes since there is a positive relationship between concentrations and discharge. The overestimation of DOC concentrations and consequently of DOC fluxes could be due to high DOC leaching.

The overestimation of DOC fluxes can also be due to the fact we choose to not recalibrate the hydrology scheme but instead we optimized the model for the discharge by adjusting the surface roughness of the vegetation (section 2.2.1). Since those four stations are all located in the same region with the same type of land cover (Western Europe), two other locations have been selected: England and the Baltic Sea. For those two locations, there are no time series data for DOC flux but some studies have measured DOC concentrations/fluxes. Worrall et al. (2012) estimated DOC concentration across UK and Fransner et al. (2016) reported modelled DOC concentrations for all the catchments flowing into the Baltic Sea.

Finally, although the model-data comparison points to a slight overestimation of the river DOC export flux, our pan-European estimate amounts to 12.3 TgC yr$^{-1}$. This estimate is in fact about 35 % lower than the one reported in another model study by Li et al. (2019), based on TRIPLEX-HYDRA, a process-based model for which the DOC export flux reaches 19.3 TgC yr$^{-1}$. Li et al. (2019) applied the model at the global scale and simulation results were primarily evaluated against observations in the world-largest rivers and for Europe only included the Volga River. Li et al. (2019) then applied the model for multiple rivers in Europe such as the Danube, the Po, and the Elbe. Despite these different scales of analysis, the export fluxes predicted by both models fall within the same order of magnitude.

### 3.1.6 Manure implementation

The implementation of manure significantly affects DOC leaching from grasslands and croplands (Fig. 11) which cover more than half of the studied region. The average annual input rate of manure into the soil is around 2.5 gC m$^{-2}$ yr$^{-1}$ (Fig. 2c). With manure implementation, the DOC leaching rate increase drastically (average of +72% compared to the DOC leaching without manure), in particular in the oceanic and humid continental climate regions, where the average DOC leaching rate changes from 1.6 to 2.7 gC m$^{-2}$ yr$^{-1}$ and 1.7 to 2.5 gC m$^{-2}$ yr$^{-1}$, respectively. For the whole of Europe, manure implementation leads to an increase of total DOC leaching into the river network from 9.8 to 14.3 TgC yr$^{-1}$ (fig 11 (a-b)). Figure 11 (d) shows that the application of manure increases DOC leaching in particular in winter (January, February and March) while in summer (July, August and September) the increase is relatively low. In ORCHILEAK, the manure derived DOC first enters the topsoil. There, a part of it is decomposed, and the rest is transported to deeper soil layers with percolating water. Finally, a variable part of the DOC derived from manure is flushed out of the soil column with the surface runoff and belowground drainage. As manure enters first the topsoil, one could expect that it would increase mainly the DOC leaching from the top-soil. However, our results show that the application of manure does not influence the ratio of DOC leaching through surface runoff vs. belowground drainage. Over Europe, the average increase in top-soil DOC leaching due to manure is equal to half of the total increase, the rest of the increase being contributed by the drainage.
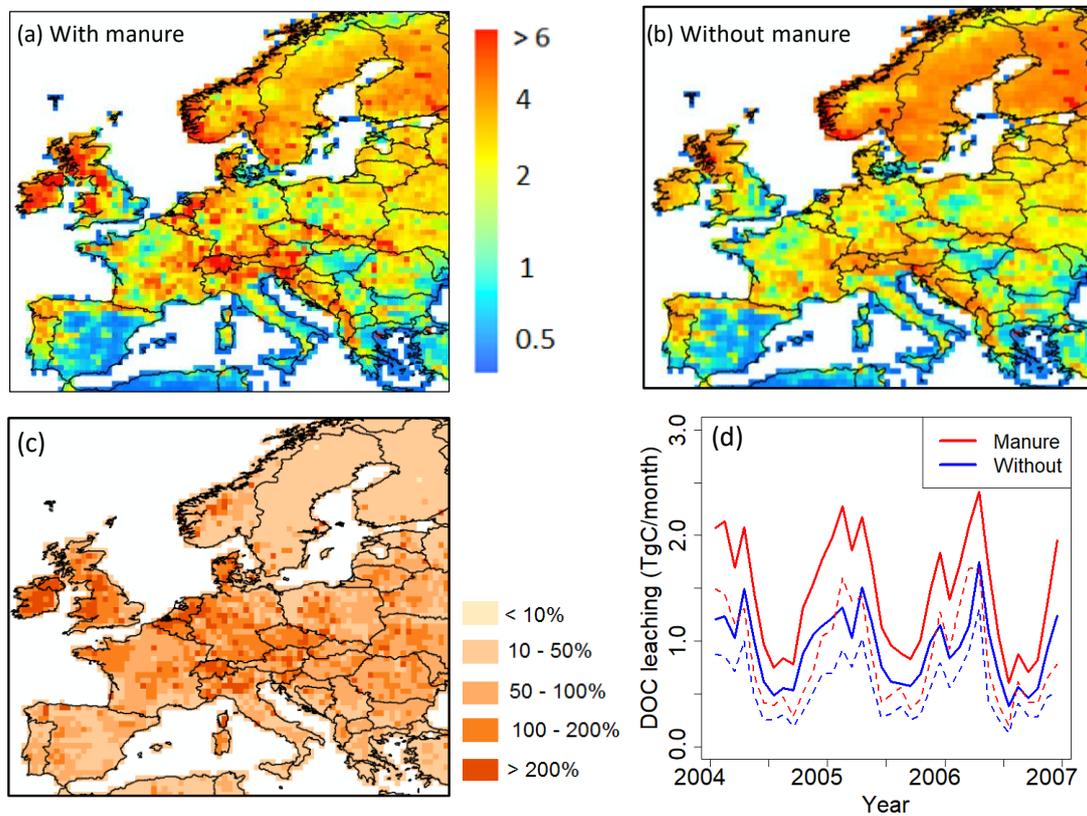
**Figure 11. Comparison of modeled yearly mean terrestrial DOC leaching flux (period 1979-2006) to the river European river network (in gC m$^{-2}$ yr$^{-1}$), with (a) and without (b) the representation of manure application. (c) Increase of DOC leaching in percentage compared to DOC leaching without the manure implementation. (d) Comparison of total DOC leaching (solid line) and DOC leaching through runoff only (dashed line) over all of Europe with and without manure application (years 2004-2006).**

## 3.2 European-scale DOC leaching dynamics

### 3.2.1 Drivers of DOC leaching

Here, we analyze what controls the spatial distribution and temporal variability in DOC leaching. While the grid cell and the basin scales were the most relevant for the model evaluation, when searching for potential drivers of soil DOC leaching, such as temperature, runoff and drainage (driven by precipitation), a climatologic segmentation of the European domain can help to better explain the impact of these drivers. Figure 12 shows seasonal variability of DOC leaching and total runoff (surface runoff plus drainage) in different climate zones of Europe, revealing a clear and consistent relationship between those two fluxes. The seasonal peak in DOC leaching consistently occurs in winter while minimum values are found during summer. These results suggest that both spatial and temporal variability in leaching are correlated to total runoff.
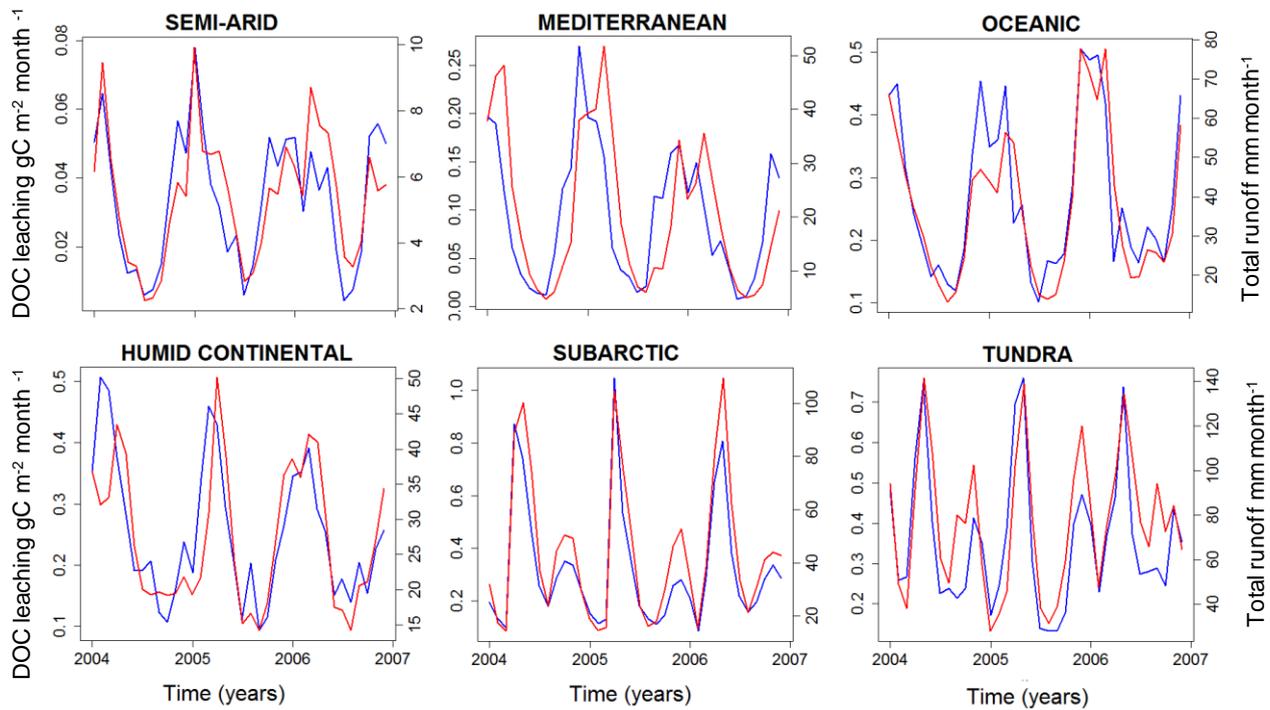
**Figure 12. Simulated DOC leaching flux (gC m$^{-2}$ month$^{-1}$) (blue) and total runoff (mm per month) (red) for the six largest climate zones in Europe (period 2004-2006).**

680

To further explore the environmental controls of the DOC leaching, we calculate the partial correlation factor for surface runoff, drainage, temperature and NPP and they are respectively 0.43, 0.54, -0.17 and 0.18, highlighting that surface runoff and drainage can explain most of the spatio-temporal variability in DOC leaching fluxes, temperature and NPP only playing a subordinate role. We decided to express DOC leaching as fraction of the annual terrestrial NPP (Figure 13). Doing this, we
685 assume that NPP, which is undoubtedly the ultimate C source for DOC production (since litter and SOC stocks, the sources of DOC, are fed by NPP), is as well an important control of the DOC leaching flux. Moreover, normalizing DOC leaching by NPP, we strive to show the possible influence of other controls, allowing for a more in-depth analysis of the effect of hydrology and climate on the DOC leaching flux. Figure 13 reveals that the fraction of terrestrial NPP lost to DOC leaching increases, as expected, with total runoff. Moreover, this fraction increases with the contribution of surface runoff to total
690 water loss from surface runoff plus drainage (Fig. 13b). This can be explained by the general decrease in soil DOC concentrations with depth (Fig. 6), leading to higher DOC concentrations in surface runoff than in drainage. In fact, according to our simulations, 97% of the leached DOC is concentrated in the surface runoff. Note that higher total runoff is often associated with a higher contribution of surface runoff, which leads to a 'flushing effect' where high runoff events contribute a disproportionate high fraction of the long-term DOC leaching (Idir et al. 1999, Raymond and Saiers 2010).
695 Finally, we found higher leaching to NPP ratios at lower temperatures (Fig. 13a), suggesting that lower temperatures lead to longer turnover times of DOC in the soil, and thus higher concentrations in the leaching flux (section 2.1.2).
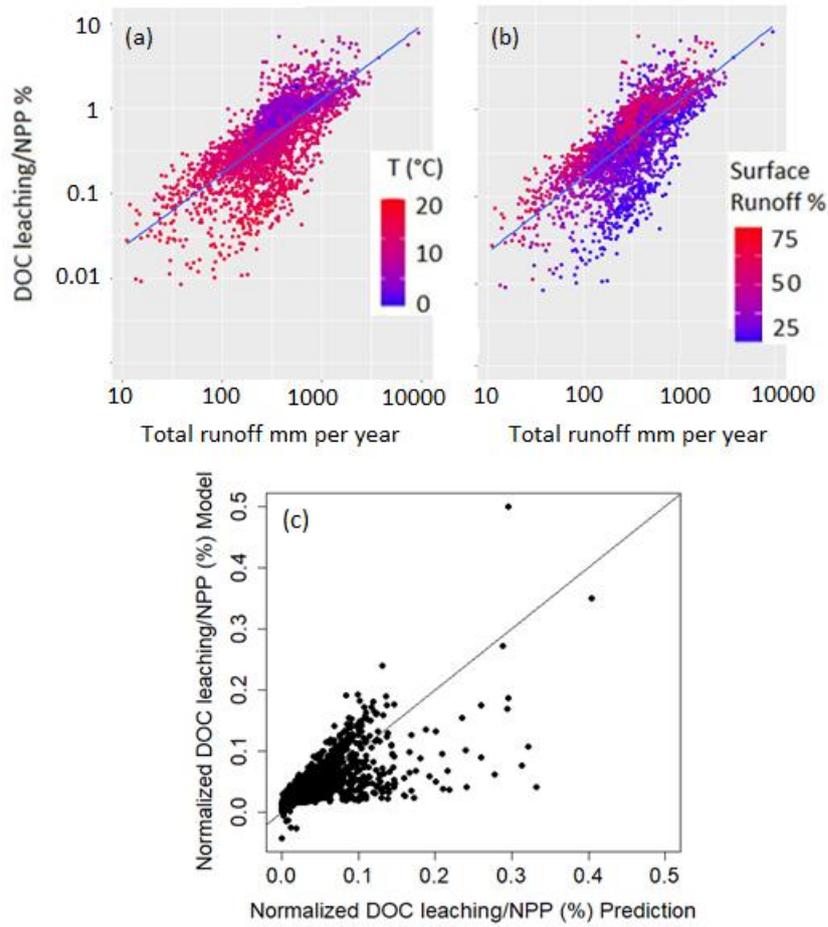
**Figure 13. Fraction (%) of terrestrial NPP that is leached as DOC in the river network as a function of total runoff. Each point represents the grid-cell average of both metrics for the entire simulation period (1979-2006). In panel (a) the color scale represents the grid-cell average temperature (°C) while in panel (b), the color scale represents the ratio of surface runoff to total runoff in percentage. Panel (c) shows the normalized predicted DOC leaching flux to NPP ratio (equation 13) against the normalized simulated values.**

To better quantify the effects of all these drivers on DOC leaching, we fitted a multi-linear regression model to predict the ratio of DOC leaching to NPP as a function of surface runoff, drainage and temperature at all grid points and for each month over the simulation period (eq. 13). The idea behind this rationale is to highlight that once normalized to the terrestrial NPP, we can directly analyse which physical drivers impact the fraction of NPP that is lost to leaching from terrestrial ecosystems. To compare the importance of each predictor for the spatiotemporal patterns of DOC leaching, we normalized all variables, Vs, of equation 13 according to equation 14 (where i is the cell index).

$$\frac{DOC\ leaching}{NPP} = K_0 + K_R * Runoff + K_D * Drainage + K_T * e^{T(°C)} \qquad (13)$$

$$K_0 = 0.01 \pm 7 * 10^{-4}$$
$$K_R = 0.342 \pm 0.009$$
$$K_D = 0.276 \pm 0.014$$
$$K_T = -0.055 \pm 0.013$$

(p-value $< 2*10^{-16}$ except for temperature where p-value $= 2.7*10^{-5}$)

$$V_{i,N} = \frac{V_i - V_{min}}{V_{max} - V_{min}} \qquad (14)$$

To rule out any significant multi-collinearity in the regression model, we calculated for each predictor the Variance Inflation Factor (VIF). The VIF evaluates the correlations among all predictors which could impact the robustness of the regression

model (James et al., 2017). The closer the VIF is to 1, the more robust is the model. In our regression, VIF's of the runoff, drainage and temperature are respectively 1.13, 1.13 and 1.01, confirming that our prediction is robust and not biased by high multicollinearity.

In Fig. 13 (c), the DOC leaching simulated by ORCHILEAK is compared with the one predicted by equation 13. Our simple regression model is able to reproduce the simulations with a residual standard error of 0.68% and a $R^2$ of 0.45. The coefficients of our regression model reveal that spatio-temporal variability in DOC leaching is mainly driven by the surface runoff ($K_R$) and drainage ($K_D$). Air temperature as third control of DOC leaching is of subordinate importance as reflected by its low predictor's coefficient ($K_T$).

Table 4 summarizes, for each climate zone in Europe, the DOC leaching fluxes (in absolute value and normalized by the NPP) as well as other important components of the terrestrial C budget. Since runoff and temperature were identified as the controlling factors of the DOC leaching flux, normalized DOC leaching fluxes are expected to be significantly different among climate zones. Indeed, the fraction of NPP lost to the river network as DOC is the lowest in the semi-arid region (0.13%) where annual precipitation is low (total runoff around 92 mm per year) and temperatures are high.

**Table 4. Key physical and biogeochemical characteristics of the six dominant climate zones of the European domain.**

| Variables | Unit | Semi-arid | Mediterranean | Oceanic | Humid continental | Subarctic | Tundra |
|---|---|---|---|---|---|---|---|
| Area | km² | 3.01E+11 | 8.74E+11 | 1.38E+12 | 2.11E+12 | 9.03E+11 | 1.56E+11 |
| Leaching | | 0.35 | 1.01 | 2.73 | 2.5 | 2.84 | 4.2 |
| NPP | gC m⁻² yr⁻¹ | 264.1 | 389.9 | 561.3 | 526.4 | 338.3 | 344.2 |
| HR | gC m⁻² yr⁻¹ | 175.5 | 278.6 | 390.6 | 345.7 | 255.3 | 266.9 |
| Harvest (crop) | gC m⁻² yr⁻¹ | 74.7 | 68 | 111.8 | 112.6 | 15.7 | 30.5 |
| Harvest (wood) | gC m⁻² yr⁻¹ | 5.4 | 25 | 46.1 | 40.7 | 41 | 41.8 |
| LUC | gC m⁻² yr⁻¹ | -0.04 | -4.8 | -5.3 | -7.7 | -15.9 | -3.7 |
| NEE calculated | gC m⁻² yr⁻¹ | 87 | 107.5 | 160 | 175 | 82.1 | 73.7 |
| Leaching/NPP | % | 0.13 | 0.26 | 0.49 | 0.48 | 0.84 | 1.22 |
| Leaching/NEE | % | 0.4 | 0.94 | 1.71 | 1.43 | 3.46 | 5.7 |
| Runoff | Mm yr⁻¹ | 30 | 63 | 82 | 91 | 236 | 404 |
| Drainage | Mm yr⁻¹ | 62 | 229 | 406 | 236 | 290 | 517 |
| Temperature | °C | 15 | 14.6 | 10.4 | 7.8 | 1.8 | 4.6 |

730

The highest fraction of NPP exported to rivers as DOC is found in the tundra climate and reach 1.22%. That can be explained by high runoff and drainage (reaching 920 mm per year) in this climate zone, but also by low temperatures lowering the fraction of DOC already decomposed within the soil column. The subarctic climate also presents a similarly high DOC leaching to NPP ratio with a value of 0.84%. The Mediterranean, Oceanic and humid continental climate zones present intermediate DOC leaching to NPP ratios of respectively 0.26%, 0.48% and 0.49%. Averaged over the whole of the EU-27, the DOC leaching flux normalized to the NPP amounts to 0.60 %.

### 3.2.2 Comparison with previous assessments of DOC leaching

In one of the first studies on the terrestrial C budget of Europe (Janssens et al., 2003) an imbalance (missing sink) between atmospheric $CO_2$ inversions and bottom-up C stock change accounting was partly attributed to the loss of carbon from land to rivers in the form of DOC of around 4 gC m$^{-2}$ yr$^{-1}$. Our results, 2.6 ± 2.5 gC m$^{-2}$ yr$^{-1}$, support this hypothesis although we suggest a DOC leaching rate slightly lower than this early study. Our lower value may come from the fact that we did not simulate peatlands and organic soils which are known hotspots of DOC leaching (Leifeld and Menichetti 2018), in particular in areas such as the northern UK and Scandinavia. Uncertainties in the processes included or omitted in the model could also explain some of the discrepancy. In terms of temporal variability, we found the highest DOC leaching in winter averaged over the continent (8.9 TgC in total for the six months of winter October to March) and the lowest in summer (5.4 TgC over the period April to September), consistent with the findings of Kindler et al. (2011). In terms of drivers of the DOC leaching fluxes, our results are in line with empirical findings by Gielen et al. (2011) that identified hydrology as the main driver of the inter- and intra-annual variability in DOC leaching. Similar conclusions have also been drawn by other empirical studies (Michalzik et al., 2001, Neff and Asner 2001, Worrall and Burt 2007).

It is also interesting to compare our results with recent global and regional model studies of DOC leaching in tropical and boreal ecosystems. For the Amazon and Congo basins, Hastie et al. (2019, 2021) found that 12 and 4 % of the NPP is exported each year to inland waters in the form of DOC and $CO_2$, respectively – much higher than the one we report for Europe (0.6%) but this value only accounts for DOC. Note that for these tropical lowland river basins extensive riparian wetlands are an important source of DOC, which are of minor importance in Europe. For the Lena river basin located in the boreal region, Bowring et al. (2020) found a DOC leaching of NPP ratio of about 1.5%. In our model assessment, this ratio reaches a very similar value of 1.2% for the boreal portion of Europe. For the temperate zone, a ratio of 0.35% for the East Coast of the US can be calculated when dividing the average DOC leaching flux of 2.7 gC m$^{-2}$ yr$^{-1}$ simulated by Tian et al. (2015) by the average NPP of 780 gC m$^{-2}$ yr$^{-1}$ estimated by Zhao et al. (2005). Further, our value is quite similar to the one extracted from the global study by Nakhavali et al. (2020) that amounts to 0.5 % for the European domain only. Overall, this comparison highlights that in Europe, the fraction of NPP lost as DOC to the river network is significantly smaller than in other regions of the world. The lower value is likely due to the lower connectivity between terrestrial and aquatic systems due to the lack of extensive wetlands, which have been reduced by major regulation of the European river network.

### 3.2.3 Implications for the terrestrial carbon budget of Europe

The terrestrial carbon budget is controlled by NPP, heterotrophic respiration, crop and wood harvesting and land use change. Here we look at the net ecosystem exchange (NEE) which is the net C exchange between land and atmosphere (Kramer et al., 2002). However, this view neglects the leakiness of terrestrial ecosystems that permanently removes a fraction of the land C and export it to the river network. Moreover, we can argue that DOC leaching represents a fraction of NEE, while the remainder of NEE can be attributed to harvest, land use change and changes in biomass and soil C stocks. From 1979 to 2012, the average NEE in Europe is 860 TgC yr$^{-1}$ (123 gC m$^{-2}$ yr$^{-1}$), equalling about 28% of the total NPP (Fig. 14b). The

ratio of DOC leaching to NEE shows drastic spatial variation, varying from an average value of 0.4% in the semi-arid region to a value of 5.7% in the tundra region. For the whole Europe, the DOC leaching is about 3% of the NEE.
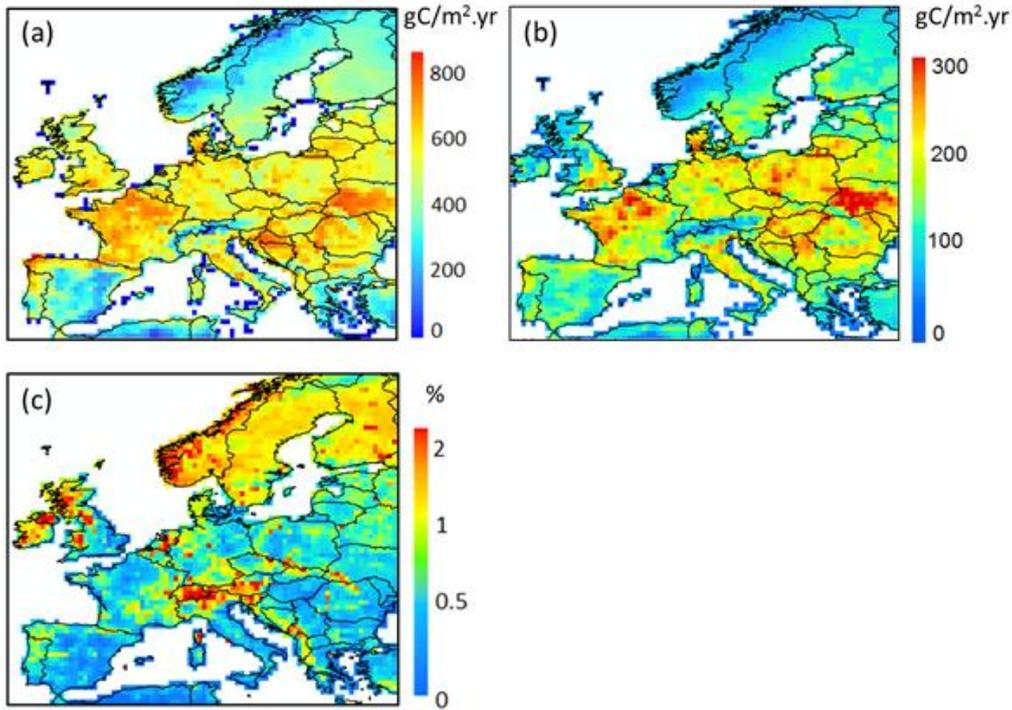
775   **Figure 14. Grid-cell average of (a) Net Primary Production (NPP), (b) Net Ecosystem Exchange (NEE) and (c) fraction of NPP leached to the river network as DOC (%) for the period 1979-2006**

### 3.3 Model limitations

ORCHILEAK is a LSM that simulates the impact of riverine DOC transfers on the terrestrial C budget, but it still suffers from several limitations. In fact, ORCHILEAK cannot represent all biogeochemical transformation processes affecting DOC
780   in the soil column and the river network (Lauerwald et al., 2017). For instance, environmental controls such as soil pH and ionic strength have been demonstrated to have an impact on DOC solubility in soils (Monteith et al., 2007) and thus affect DOC leaching to streams. Unfortunately, these processes are not represented in our model, as there are still no reliable methods and forcing data to simulate the dynamics of soil pH and ionic strength in the soil solution at large scale.

As mentioned before, peatlands are not included in the model, yet they cover a large part of Northern Europe. Peatlands are
785   known to play an important role in  the C cycle, and are an important source of DOC to the river network. One of the major next steps would thus be to merge ORCHILEAK with ORCHIDEE-PEAT, a new branch of the land surface model ORCHIDEE simulating the development and C balance of peatlands (Qiu et al., 2019).

Another source of DOC originates from wastewater treatments plants that are not included in the model due to the lack of forcing data related to the sewage water treatment. It has been shown that DOC concentrations in sewage are important
790   (Griffith et al 2009). However, Meybeck (1986) showed that DOC from sewage is very labile and only affects the concentration within short distances downstream of water processing plants. Having avoided observation data from sites known to be impacted by sewage effluents directly, we assume that our model-data evaluation was not impacted by this potential DOC source. For assessing the role of soil DOC leaching in the terrestrial C budget, sewage is not a contribution of direct interest.

795   While riparian zones are a major source of DOC to the river network (Inamdar and Mitchell 2006, Grabs et al. 2012), the impact of riparian zones on DOC leaching through runoff to the river network is only implicitly represented in the model (as described in Lauerwald et al. 2017). Due to the coarse resolution of the model, riparian zones around small streams (order 1 to 3) cannot be explicitly included in the model. It is assumed that the extent of the riparian zones, from which most of the

DOC stems, scales linearly to the surface area of these small streams, both in time as well as in space (i.e. between different grid cells of our model grid). While the surface area of these small streams is not directly represented, Lauerwald et al. (2017) assumed that spatial and temporal variations in this stream surface area scales to the square root of discharge that is flowing through these streams, roughly in line with empirical scaling laws (e.g. Raymond et al. 2012). For the larger rivers, for which the surface area is explicitly represented in the model, it is assumed that the inundated riparian zone can temporally make up to 10% of the river water surface area, depending on the temporal variability of discharge. Here, DOC produced from decomposition of litter and SOC is directly injected into the river water body.

ORCHILEAK could further be improved through the implementation of lakes and reservoirs. It has been shown that dams have a direct impact on C retention efficiency in the inland water river network (Maavara et al., 2017). So far, ORCHILEAK does not represent lateral transport of POC at continental scale, yet its non-negligible role in the terrestrial C budget has been demonstrated (Zhang et al. 2018; 2020, Naipal et al. 2019). Finally, the effect of nutrient limitation on the C cycle is not yet account for in ORCHILEAK. It has been demonstrated that the implementation of nitrogen (N) and phosphorus (P) could reduce the simulated land C sink (Goll et al. 2012, Sun et al. 2021). It can be assumed that nutrient limitation would similarly affect DOC leaching, and could dampen its increase with rising atmospheric $CO_2$ levels predicted by previous studies with ORCHILEAK (Lauerwald et al. 2020, Hastie et al. 2021).

**4 Conclusion**

We reconstructed the terrestrial and riverine C fluxes in Europe during the period 1979-2012 using the ORCHILEAK LSM. The total C leaching from soil to European rivers is 14.3 TgC yr$^{-1}$ on average, about 0.6 % of the estimated NPP and 3% of the terrestrial net up-take of atmospheric C. This flux shows large spatial and temporal variations. In specific, DOC leaching overall increases from warm and dry regions to cold and wet regions. However, since the model does not represent peatlands yet, the simulation results for subarctic and tundra regions in northern Europe could be biased. For the whole of Europe, DOC leaching rate is the highest in winter and lowest during the summer, mainly controlled by the seasonal variation of runoff. The implementation of manure lead to a significant increase in DOC leaching over the oceanic and humid continental region where croplands and grasslands are dominant. Our results contribute to a better assessment of the land-ocean C fluxes in Europe and to a better understanding of the effects of lateral C transfer on the terrestrial C budget. Combined with recent large-scale studies in tropical and boreal biomes as well as along the east coast of the US, an emergent view regarding the global role of DOC leaching on the terrestrial C balance and its underlying drivers is progressively emerging.

**Code and data availability**

The model code used in this study is available at DOI : 10.14768/75AC2F47-4691-46AF-9B12-B1A9629CBC56

All forcing data set are listed in table 1. Data of observed discharge used in this study are available from the Global Runoff Data Center (GRDC) at www.bafg.de/GRDC. Data of observed DOC concentrations in France are provided by eau de France at http://www.data.eaufrance.fr/.

**Supplement**

The supplement related to this article is available in the attached file (pdf).

**Author contribution**

CG, RL, PR, PC designed the study. CG performed calibration and evaluation of the model, ran the simulations, and wrote the initial manuscript. RL updated the model code of ORCHILEAK to improve representation of soil hydrology and DOC

cycling. HZ implemented the representation of manure impacts on soil DOC dynamics into the model code. All co-authors contributed to interpretation of model results and improvement of the manuscript.

**Competing interests**

The authors declare that they have no conflict of interest.

**Acknowledgements**

RL, PC and BG acknowledge funding from the French state aid managed by the ANR under the "Investissements d'avenir" programme [ANR-16-CONV-0003]. HZ, PR and RL acknowledge the 'Lateral-CNP' project (No. 34823748) supported by the Fonds de la Recherche Scientifique –FNRS. CG and PR acknowledges funding from the European Union's Horizon 2020 research and innovation programme under Grant Agreements N° 776810 (project VERIFY) and N° 101003536 (ESM 2025).

**References**

Abril G., M. Nogueira, H. Etcheber, G. Cabeçadas, E. Lemaire, M. Brogueira. Behaviour of organic carbon in nine contrasting European estuaries. Estuar. Coast. Shelf Sci., 54, pp. 241-262, 2002.

Avitabile, V., Camia, A.,. An assessment of forest biomass maps in Europe using harmonized national statistics and inventory plots. For. Ecol. Manage. 409, 489–498, 2018

Berggren, M. Al-Kharusi, E.S. Decreasing organic carbon bioreactivity in European rivers. Freshw. Biol., 65 (6), pp. 1128-1138, 10.1111/fwb.v65.610.1111/fwb.13498, 2020

Bloom, Anthony; Williams, Mathew. CARDAMOM 2001-2010 global carbon Model-Data Fusion (MDF) analysis, 2001-2010 [dataset]. University of Edinburgh. School of GeoSciences. https://doi.org/10.7488/ds/316, 2015

Bowring, S. P. K., Lauerwald, R., Guenet, B., Zhu, D., Guimberteau, M., Tootchi, A., Ducharne, A., and Ciais, P: ORCHIDEE MICT-LEAK (r5459), a global model for the production, transport, and transformation of dissolved organic carbon from Arctic permafrost regions – Part 1: Rationale, model description, and simulation protocol, Geosci. Model Dev., 12, 3503–3521, https://doi.org/10.5194/gmd-12-3503-2019, 2019.

Bowring, S. P. K., Lauerwald, R., Guenet, B., Zhu, D., Guimberteau, M., Regnier, P., Tootchi, A., Ducharne, A., and Ciais, P.: ORCHIDEE MICT-LEAK (r5459), a global model for the production, transport, and transformation of dissolved organic carbon from Arctic permafrost regions – Part 2: Model evaluation over the Lena River basin, Geosci. Model Dev., 13, 507–520, https://doi.org/10.5194/gmd-13-507-2020, 2020.

Camino-Serrano, M., Gielen, B., Luyssaert, S., Ciais, P., Vicca, S., Guenet, B., Vos, B. De, Cools, N., Ahrens, B., Altaf Arain, M., Borken, W., Clarke, N., Clarkson, B., Cummins, T., Don, A., Pannatier, E. G., Laudon, H., Moore, T., Nieminen, T. M., Nilsson, M. B., Peichl, M., Schwendenmann, L., Siemens, J., and Janssens, I.: Linking variability in soil solution dissolved organic carbon to climate, soil type, and vegetation type, Global Biogeochem. Cy., 28, GB004726, https://doi.org/10.1002/2013gb004726, 2014.

Camino-Serrano, M., Guenet, B., Luyssaert, S., Ciais, P., Bastrikov, V., De Vos, B., Gielen, B., Gleixner, G., Jornet-Puig, A., Kaiser, K., Kothawala, D., Lauerwald, R., Peñuelas, J., Schrumpf, M., Vicca, S., Vuichard, N., Walmsley, D., and Janssens, I. A.: ORCHIDEE-SOM: modeling soil organic carbon (SOC) and dissolved organic carbon (DOC) dynamics along vertical soil profiles in Europe, Geosci. Model Dev., 11, 937–957, https://doi.org/10.5194/gmd-11-937-2018, 2018.

885

Campoy, A., Ducharne, A., Cheruy, F., Hourdin, F., Polcher, J., and Dupont, J. C.: Response of land surface fluxes and precipitation to different soil bottom hydrological conditions in a general circulation model, J. Geophys. Res.-Atmos., 118, 10725–10739, https://doi.org/10.1002/Jgrd.50627, 2013.

890    Ciais, P., et al. (2013), Carbon and other biogeochemical cycles, in Climate Change: The Physical Science Basis. Contribution of Working Group I to the Fifth Assessment Report of the Intergovernmental Panel on Climate Change, edited by T. F. Stocker et al., Cambridge Univ. Press, Cambridge, U. K., and New York, 2013.

Cole, J.J., Prairie, Y.T., Caraco, N.F., McDowell, W.H., Tranvik, L.J., Striegl, R.G., Duarte, C.M., Kortelainen, P.,
895    Downing, J.A., Middelburg, J.J., Melack, J.: Plumbing the global carbon cycle: integrating inland waters into the terrestrial carbon budget. Ecosystems 10 (1), 171–184, 2007.

Delpla I, Baures E, Jung AV, Thomas O. Impacts of rainfall events on runoff water quality in an agricultural environment in temperate areas. Sci Total Environ. 409(9): 1683–8. https://doi.org/10.1016/j.scitotenv.2011.01.033, 2011.

900

Drake, T. W., P. A. Raymond, and R. G. M. Spencer.Terrestrial carbon inputs to inland waters: a current synthesis of estimates and uncertainty. Limnology and Oceanography Letters 3:132–142. http://doi.org/10.1002/lol2.1005, 2018.

FAO/IIASA/ISRIC/ISS-CAS/JRC. Harmonized World Soil Database (version 1.2). FAO, Rome, Italy and IIASA,
905    Laxenburg, Austria, 2012

Farjalla VF, Marinho CC, Faria BM, Amado AM, Esteves FA, Bozelli RL, Giroldo D: Synergy of fresh and accumulated organic matter to bacterial growth. Microb Ecol 57(4):657–666. doi: 10.1007/s00248-008-9466-8, 2009.

910    Fonte ES, Amado AM, Meirelles-Pereira F, Esteves FA, Rosado AS, Farjalla VF: The combination of different carbon sources enhances bacterial growth efficiency in aquatic ecosystems. Microb Ecol 66(4):871–878. doi:10.1007/s00248-013-0277-1, 2013.

Fransner F, Nycander J, Mörth C-M et al: Tracing terrestrial DOC in the Baltic Sea—a 3-D model study. Global
915    Biogeochem Cycle 30:134–148. doi:10.1002/2014GB005078, 2016.

Friedlingstein P., O'Sullivan M., Jones M.W. , Andrew R.M. , Hauck J., Olsen A., et al. Global carbon budget 2020. Earth Syst Sci Data, 12, pp. 3269-3340, 10.5194/essd-12-3269-2020, 2020.

920    Gielen, B., Neirynck, J., Luyssaert, S., and Janssens, I. A.: The importance of dissolved organic carbon fluxes for the carbon balance of a temperate Scots pine forest, Agr. Forest Meteorol.,151, 270–278, https://doi.org/10.1016/j.agrformet.2010.10.012, 2011.

Goll, D. S., Brovkin, V., Parida, B. R., Reick, C. H., Kattge, J., Reich, P. B., van Bodegom, P. M., and Niinemets, Ü.: Nutrient limitation reduces land carbon uptake in simulations with a model of combined carbon, nitrogen and phosphorus cycling, Biogeosciences, 9, 3547–3569, https://doi.org/10.5194/bg-9-3547-2012, 2012.

Goll, D. S., Vuichard, N., Maignan, F., Jornet-Puig, A., Sardans, J., Violette, A., Peng, S., Sun, Y., Kvakic, M., Guimberteau, M., Guenet, B., Zaehle, S., Penuelas, J., Janssens, I., and Ciais, P.: A representation of the phosphorus cycle for ORCHIDEE (revision 4520), Geosci. Model Dev., 10, 3745-3770, https://doi.org/10.5194/gmd-10-3745-2017, 2017.

Goll, D. S., Joetzjer, E., Huang, M., and Ciais, P.: Low phosphorus availability decreases susceptibility of tropical primary productivity to droughts, Geophys. Res. Lett., 45, 8231–8240, https://doi.org/10.1029/2018GL077736, 2018. Qiu, C., Zhu, D., Ciais, P., Guenet, B., Peng, S., Krinner, G., Tootchi, A., Ducharne, A., and Hastie, A.: Modelling northern peatland area and carbon dynamics since the Holocene with the ORCHIDEE-PEAT land surface model (SVN r5488), Geosci. Model Dev., 12, 2961–2982, https://doi.org/10.5194/gmd-12-2961-2019, 2019.

Grabs, Thomas, et al. "Riparian zone hydrology and soil water total organic carbon (TOC): implications for spatial variability and upscaling of lateral riparian TOC exports." Biogeosciences 9.10: 3901-3916, 2012.

Griffith, David R., Rebecca T. Barnes, and Peter A. Raymond. "Inputs of fossil carbon from wastewater treatment plants to US rivers and oceans." Environmental Science & Technology 43.15: 5647-5651, 2009.

Guimberteau, M., Drapeau, G., Ronchail, J., Sultan, B., Polcher, J., Martinez, J.-M., Prigent, C., Guyot, J.-L., Cochonneau, G., Es- pinoza, J. C., Filizola, N., Fraizy, P., Lavado, W., De Oliveira, E., Pombosa, R., Noriega, L., and Vauchel, P.: Discharge sim- ulation in the sub-basins of the Amazon using ORCHIDEE forced by new datasets, Hydrol. Earth Syst. Sci., 16, 911–935, https://doi.org/10.5194/hess-16-911-2012, 2012.

Guimberteau, M., Zhu, D., Maignan, F., Huang,Y.,Yue, C., Dantec- Nédélec, S., Ottlé, C., Jornet-Puig, A., Bastos, A., Laurent, P., Goll, D., Bowring, S., Chang, J., Guenet, B., Tifafi, M., Peng, S., Krinner, G., Ducharne, A., Wang, F., Wang, T., Wang, X., Wang, Y., Yin, Z., Lauerwald, R., Joetzjer, E., Qiu, C., Kim, H., and Ciais, P.: ORCHIDEE-MICT (v8.4.1), a land surface model for the high latitudes: model description and validation, Geosci. Model Dev., 11, 121–163, https://doi.org/10.5194/gmd-11-121- 2018, 2018.

Hartmann, J., Lauerwald, R., and Moosdorf, N.: A brief overview of the GLObal RIver CHemistry Database, GLORICH, Procedia, Earth Planet. Sci., 10, 23–27, 2014.

Hastie, A., Lauerwald, R., Ciais, P., Regnier, P. Aquatic carbon fluxes dampen the overall variation of net ecosystem productivity in the Amazon basin: An analysis of the interannual variability in the boundless carbon cycle. Global Change Biology, 25: 2094– 2111. https://doi.org/10.1111/gcb.14620, 2019.

Hastie, A., Lauerwald, R., Ciais, P., Papa, F., and Regnier, P.: Historical and future contributions of inland waters to the Congo basin carbon balance, Earth Syst. Dynam., 12, 37–62, https://doi.org/10.5194/esd-12-37-2021, 2021.

Humbert, G., Parr, T.B., Jeanneau, L. et al. Agricultural Practices and Hydrologic Conditions Shape the Temporal Pattern of Soil and Stream Water Dissolved Organic Matter. Ecosystems 23, 1325–1343. https://doi.org/10.1007/s10021-019-00471-w, 2020

Idir, S., A.Probst, D.Viville, and J. L.Probst, Contribution of saturated areas and hillslopes to the water and element fluxes exported during a storm event: Tracing with dissolved organic carbon and silica. The Strengbach catchment case study (Vosges, France), *C. R. Acad. Sci., Ser. II*, **328**(2), 89– 96, doi:10.1016/s1251-8050(99)80003-2, 1999.

970 Inamdar, Shreeram P., and Myron J. Mitchell. "Hydrologic and topographic controls on storm-event exports of dissolved organic carbon (DOC) and nitrate across catchment scales." Water Resources Research 42.3, 2006.

James, Gareth; Witten, Daniela; Hastie, Trevor; Tibshirani, Robert. An Introduction to Statistical Learning (8th ed.). Springer Science+Business Media New York. ISBN 978-1-4614-7138-7, 2017.

975 Janssens, I. A., Freibauer, A., Ciais, P., Smith, P., Nabuurs, G. J., Folberth, G., Schlamadinger, B., Hutjes, R. W. A., Ceulemans, R., Schulze, E. D., Valentini, R., and Dolman, A. J.: Europe's terrestrial biosphere absorbs 7 to 12% ofeuropean anthropogenic CO2 emissions, Science, 300, 1538–1542, 2003

Kalbitz, K., Schmerwitz, J., Schwesig, D., and Matzner, E.: Biodegradation of soil-derived dissolved organic matter as
980 related to its properties, Geoderma, 113, 273–291, 2003.

Kicklighter DW, et al. Insights and issues with simulating terrestrial DOC loading of Arctic river networks. Ecol Appl 23(8):1817–1836, 2013.

985 Kindler, R., Siemens, J., Kaiser, K., Walmsley, D. C., Bernhofer, C., Buchmann, N., Cellier, P., Eugster, W., Gleixner, G., Grunwald, T., Heim, A., Ibrom, A., Jones, S. K., Jones, M., Klumpp, K., Kutsch, W., Larsen, K. S., Lehuger, S., Loubet, B., Mckenzie, R., Moors, E., Osborne, B., Pilegaard, K., Rebmann, C., Saunders, M., Schmidt, M. W. I., Schrumpf, M., Seyfferth, J., Skiba, U., Soussana, J.-F., Sutton, M. A., Tefs, C., Vowinckel, B., Zeeman, M. J., and Kaupenjohann, M. Dissolved carbon leaching from soil is a crucial component of the net ecosystem carbon balance, Glob. Change Biol., 17,
990 1167–1185, https://doi.org/10.1111/j.1365-486.2010.02282.x, 2011.

Köchy, M., Hiederer, R., & Freibauer, a. Global distribution of soil organic carbon – Part 1: Masses and frequency distributions of SOC stocks for the tropics, permafrost regions, wetlands, and the world. *Soil*, *1*(1), 351–365. https://doi.org/10.5194/soil-1-351-2015, 2015.
995
Kramer K, Leinonen I, Bartelink HH et al. Evaluation of six process-based for- est growth models using eddy-covariance measurements of CO(2) and H(2)O fluxes at six forest sites in Europe. Global Change Biology, 8, 213–230, 2002.

Krinner, G. et al. A dynamic global vegetation model for studies of the coupled atmosphere-biosphere system. Global
1000 Biogeochem. Cycles 19**,** 1–33, 2005.

Lauerwald, R., Hartmann, J., Ludwig, W. & Moosdorf, N. Assessing the nonconservative fluvial fluxes of dissolved organic carbon in North America. *J. Geophys. Res.* **117**, G01027, 2012.

1005 Lauerwald, R., Laruelle, G. G., Hartmann, J., Ciais, P., & Regnier, P. A. G. Spatial patterns in CO2 evasion from the global river network. Global Biogeochemical Cycles, 29(5), 534–554. https://doi. org/10.1002/2014GB004941, 2015

Lauerwald, R., Regnier, P., Camino-Serrano, M., Guenet, B., Guimberteau, M., Ducharne, A., … Ciais, P. ORCHILEAK (revision 3875): a new model branch to simulate carbon transfers along the terrestrial--aquatic continuum of the Amazon basin. Geoscientific Model Development, 10(10), 3821–3859. https://doi.org/10.5194/gmd-10-3821-2017, 2017.

Lauerwald, R., Regnier, P., Guenet, B., Friedlingstein, P., Ciais, P. How simulations of the land carbon sink are biased by ignoring fluvial carbon transfers –A case study for the Amazon basin, Volume 3, Issue 2, 21 August 2020, Pages 226-236 https://doi.org/10.1016/j.oneear.2020.07.009, 2020

Lehner B, Verdin K, Jarvis A. New global hydrography derived from spaceborne elevation data. *EOS, Transactions of the American Geophysical Union* **89**: 93– 104, 2008.

Leifeld, J., & Menichetti, L. The underappreciated potential of peatlands in global climate change mitigation strategies /704/47/4113 /704/106/47 article. Nature Communications, 9(1). https://doi.org/10.1038/s41467-018-03406-6, 2018.

Le Quéré, C., Moriarty, R., Andrew, R. M., Peters, G. P., Ciais, P., Friedlingstein, P., Jones, S. D., Sitch, S., Tans, P., Arneth, A., Boden, T. A., Bopp, L., Bozec, Y., Canadell, J. G., Chini, L. P., Chevallier, F., Cosca, C. E., Harris, I., Hoppema, M., Houghton, R. A., House, J. I., Jain, A. K., Johannessen, T., Kato, E., Keel- ing, R. F., Kitidis, V., Klein Goldewijk, K., Koven, C., Landa, C. S., Landschützer, P., Lenton, A., Lima, I. D., Marland, G., Mathis, J. T., Metzl, N., Nojiri, Y., Olsen, A., Ono, T., Peng, S., Peters,W., Pfeil, B., Poulter, B., Raupach, M. R., Regnier, P., Rö- denbeck, C., Saito, S., Salisbury, J. E., Schuster, U., Schwinger, J., Séférian, R., Segschneider, J., Steinhoff, T., Stocker, B. D., Sutton, A. J., Takahashi, T., Tilbrook, B., van der Werf, G. R., Viovy, N.,Wang, Y.-P.,Wanninkhof, R.,Wiltshire, A., and Zeng, N.: Global carbon budget 2014, Earth Syst. Sci. Data, 7, 47–85, https://doi.org/10.5194/essd-7-47-2015, 2015.

Le Quéré, C., Andrew, R. M., Friedlingstein, P., Sitch, S., Pongratz, J., Manning, A. C., Korsbakken, J. I., Peters, G. P., Canadell, J. G., Jackson, R. B., Boden, T. A., Tans, P. P., Andrews, O. D., Arora, V. K., Bakker, D. C. E., Barbero, L., Becker, M., Betts, R. A., Bopp, L., Chevallier, F., Chini, L. P., Ciais, P., Cosca, C. E., Cross, J., Currie, K., Gasser, T., Harris, I., Hauck, J., Haverd, V., Houghton, R. A., Hunt, C. W., Hurtt, G., Ilyina, T., Jain, A. K., Kato, E., Kautz, M., Keeling, R. F., Klein Goldewijk, K., Körtzinger, A., Landschützer, P., Lefèvre, N., Lenton, A., Lienert, S., Lima, I., Lombardozzi, D., Metzl, N., Millero, F., Monteiro, P. M. S., Munro, D. R., Nabel, J. E. M. S., Nakaoka, S., Nojiri, Y., Padin, X. A., Peregon, A., Pfeil, B., Pierrot, D., Poulter, B., Rehder, G., Reimer, J., Rödenbeck, C., Schwinger, J., Séférian, R., Skjelvan, I., Stocker, B. D., Tian, H., Tilbrook, B., Tubiello, F. N., van der Laan-Luijkx, I. T., van der Werf, G. R., van Heuven, S., Viovy, N., Vuichard, N., Walker, A. P., Watson, A. J., Wiltshire, A. J., Zaehle, S., and Zhu, D.: Global Carbon Budget 2017, Earth Syst. Sci. Data, 10, 405–448, https://doi.org/10.5194/essd-10-405-2018, 2018.

Li, M., Peng, C., Zhou, X., Yang, Y., Guo, Y., Shi, G., & Zhu, Q. Modeling global riverine DOC flux dynamics from 1951 to 2015. Journal of Advances in Modeling Earth Systems, 11, 514–530. https://doi.org/10.1002/2018MS001363, 2019.

Maavara, T., Lauerwald, R., Regnier, P., & Van Cappellen, P. Global perturbation of organic carbon cycling by river damming. Nature Communications, 8(May), 1–10. https://doi.org/10.1038/ncomms15347, 2017

Mattsson T., P. Kortelainen, A. Laubel, D. Evans, M. Pujo-Pay, A. Raeike, P. Conan. Export of dissolved organic matter in relation to land use along a European climatic gradient. Sci. Total Environ., 407, pp. 1967-1976, 2009.

Meybeck, M. Riverine transport of atmospheric carbon: sources, global typology and budget. Water, Air and Soil Pollution 70, 443–463, 1993a

Meybeck, M. C, N, P and S in rivers: from sources to global inputs. In Interactions of C, N, P and S Biogeochemical cycles and global change (Wollast, R., Mackenzie, F. T. & Chou, L., eds). NATO ASI Series, 14. Springer-Verlag, Berlin, pp. 163–191, 1993b.

Michalzik B., Kalbitz K., Park J.H. and Matzner E. Fluxes and concentrations of dissolved organic carbon and nitrogen – a synthesis for temperate forests. Biogeochemistry 52: 173–205, 2001.

Moore, T. R., de Souza, W., and Koprivnjak, J.-F.: Controls on the sorption of dissolved organic carbon by soils, Soil Sci., 154, 120– 129, 1992.

Muñoz-SabaterJ., Dutra, E., Agustí-Panareda, A., Albergel, C., Arduini, G., Balsamo, G., Boussetta, S., Choulga, M., Harrigan, S., Hersbach, H., Martens, B., Miralles, D. G., Piles, M., Rodríguez-Fernández, N. J., Zsoter, E., Buontempo, C., and Thépaut, J.-N.: ERA5-Land: A state-of-the-art global reanalysis dataset for land applications, Earth Syst. Sci. Data,13, 4349–4383, https://doi.org/10.5194/essd-13-4349-2021, 2021.

Nakhavali, M., Friedlingstein, P., Lauerwald, R., Tang, J., Chadburn, S., Camino-Serrano, M., Guenet, B., Harper, A., Walmsley, D., Peichl, M., and Gielen, B.: Representation of dissolved organic carbon in the JULES land surface model (vn4.4_JULES-DOCM), Geosci. Model Dev., 11, 593–609, https://doi.org/10.5194/gmd-11-593-2018, 2018.

Nakhavali, M., Lauerwald, R., Regnier, P., Guenet, B., Chadburn, S., & Friedlingstein, P. Leaching of dissolved organic carbon from mineral soils plays a significant role in the terrestrial carbon balance, (June 2020), 1083–1096. https://doi.org/10.1111/gcb.15460, 2021

Nash, J. E. and Sutcliffe, J. V.: River flow forecasting through con-ceptual models, Part I - A discussion of principles, J. Hydrol., 10,282–290, 1970.

Neff J.C. and Asner G.P. Dissolved organic carbon in terrestrial ecosystems: a synthesis and a model. Ecosystems 4: 29–48, 2001.

d'Orgeval, T., Polcher, J., & de Rosnay, P. Sensitivity of the West African hydrological cycle in ORCHIDEE to infiltration processes. Hydrology and Earth System Sciences, 12, 1387– 1401. https://doi.org/10.5194/hess-12-1387-2008, 2008.

Parton, W. J., Stewart, J. W., and Cole, C. V.: Dynamics of C, N, P and S in grassland soils: a model, Biogeochemistry, 5, 109–131, https://doi.org/10.1007/bf02180320, 1988.

Peel, M. C., Finlayson, B. L., & McMahon, T. A. Updated world map of the Köppen-Geiger climate classification. *Hydrology and earth system sciences*, *11*(5), 1633-1644, 2007.

Peng, S., Ciais, P., Maignan, F., Li, W., Chang, J., Wang, T., and Yue, C.: Sensitivity of land use change emission estimates to historical land use and land cover mapping, Global Biogeochem. Cy., 31, 626–643, https://doi.org/10.1002/2015GB005360, 2017.

1095     Polcher, J.: Les processus de surface à l'échelle globale et leurs interactions avec l'atmosphère, Habilitation à diriger des recherches, University Pierre et Marie Curie, Paris, France, 2003.

Raymond PA, Saiers JE. Event controlled DOC export from forested watersheds. Biogeochemistry 100(1–3):197–209, 2010.

1100     Raymond, Peter A., et al. "Scaling the gas transfer velocity and hydraulic geometry in streams and small rivers." Limnology and Oceanography: Fluids and Environments 2.1: 41-53, 2012.

Regnier, P., Friedlingstein, P., Ciais, P., Mackenzie, F. T., Gruber, N., Janssens, I. A., Laruelle, G. G., Lauerwald, R., Luyssaert, S., Andersson, A. J., Arndt, S., Arnosti, C., Borges, A. V., Dale, A. W., Gallego-Sala, A., Goddéris, Y., Goossens,
1105     N., Hartmann, J., Heinze, C., Ilyina, T., Joos, F., Larowe, D. E., Leifeld, J., Meysman, F. J. R., Munhoven, G., Raymond, P. A., Spahni, R., Suntharalingam, P., and Thullner, M.: Anthropogenic perturba- tion of the carbon fluxes from land to ocean, Nat. Geosci., 6, 597–607, https://doi.org/10.1038/ngeo1830, 2013.

Reynolds, C., Jackson, T. & Rawls, W. Estimating available water content by linking 424 the FAO soil map of the world
1110     with global soil profile databases and pedo-transfer 425 functions. Am. Geophys. Union Fall Meet. EOS Trans. Spring Meet. Suppl. 80, S132 426, 1999.

de Rosnay, P., Polcher, J., Bruen, M., and Laval, K.: Im- pact of a physically based soil water flow and soil- plant interaction representation for modeling large-scale land surface processes, J. Geophys. Res.-Atmos., 107, 4118,
1115     https://doi.org/10.1029/2001JD000634, 2002.

Royer, I.; Angers, D. A.; Chantigny, M. H.; Simard, R. R.; Cluis, D. Dissolved organic carbon in runoff and tile-drain water under corn and forage fertilized with hog manure. J. Environ. Qual. 2007, 36, 855–863. doi: 10.2134/jeq2006.0355, 2006.

1120     Saxton KE, Rawls WJ, Romberger SJ, Papendick RI. Estimating generalized soil-water characteristics from texture. Soil Science Society of America Journal, 50, 1031–1036, 1986.

Singh, S., Dutta, S., and Inamdar, S.: Land application of poultry manure and its influence on spectrofluorometric characteristics of dissolved organic matter, Agriculture, Ecosystems and Environment, 193, 25–36,
1125     https://doi.org/10.1016/j.agee.2014.04.019, 2014.Zhang, H., Goll, D. S., Manzoni, S., Ciais, P., Guenet, B., and Huang, Y.: Modeling the effects of litter stoichiometry and soil mineral N availability on soil organic matter formation using CENTURY-CUE (v1.0), Geosci. Model Dev., 11, 4779–4796, https://doi.org/10.5194/gmd-11-4779-2018, 2018.

Sitch, S. et al., Evaluation of ecosystem dynamics, plant geography and terrestrial carbon cycling in the LPJ dynamic global
1130     vegetation model, Glob. Chang. Biol., 9(2), 161–185, doi:10.1046/j.1365-2486.2003.00569.x, 2003.

Smith, J., Gottschalk, P., Bellarby, J., Chapman, S., Lilly, A., Tow- ers, W., Bell, J., Coleman, K., Nayak, D., Richards, M., Hillier, J., Flynn, H., Wattenbach, M., Aitkenhead, M., Yeluripurti, J., Farmer, J., Milne, R., Thomson, A., Evans, C., and Smith, P.: Estimating changes in national soil carbon stocks using ECOSSE – a new model that includes upland organic
1135     soils. Part II. Application in Scotland, Clim. Res., 45, 193–205, https://doi.org/10.3354/cr00902, 2010.

Sun, Y., Goll, D. S., Chang, J., Ciais, P., Guenet, B., Helfenstein, J., Huang, Y., Lauerwald, R., Maignan, F., Naipal, V., Wang, Y., Yang, H., and Zhang, H.: Global evaluation of the nutrient-enabled version of the land surface model ORCHIDEE-CNP v1.2 (r5986), Geosci. Model Dev., 14, 1987–2010, https://doi.org/10.5194/gmd-14-1987-2021, 2021.

Tian, H., Q. Yang, R. G. Najjar, W. Ren, M. A. M. Friedrichs, C. S. Hopkinson, and S. Pan: Anthropogenic and climatic influences on carbon fluxes from eastern North America to the Atlantic Ocean: A process-based modeling study, J. Geophys. Res. Biogeosci., 120, 752–772, doi:10.1002/ 2014JG002760, 2015.

Turgeon, J.: Production and biodegradation of dissolved carbon, nitrogen and phosphorus from Canadian forest floors, McGill University, 2008.

Turner D.P., W.D. Ritts, W.B. Cohen, S.T. Gower, S.W. Running, M. Zhao, M.H. Costa, A.A. Kirschbaum, J.M. Ham, S.R. Saleska, D.E. Ahl. Evaluation of MODIS NPP and GPP products across multiple biomes. Remote Sens. Environ., 102 (3-4), pp. 282-292, 10.1016/j.rse.2006.02.017, 2006.

Vorosmarty, C. J., B. M. Fekete, M. Meybeck, and R. B. Lammers, Geo- morphometric attributes of the global system of rivers at 30-minute spa- tial resolution, J. Hydrol., 237, 17–39, 2000.

Vuichard et al., Accounting for Carbon and Nitrogen interactions in the Global Terrestrial Ecosystem Model ORCHIDEE (trunk version, rev 4999): multi-scale evaluation of gross primary production. Geosci. Model Dev. Discuss., https://doi.org/10.5194/gmd-2018-261, 2018

Wang, T., Ottle, C., Boone, A., Ciais, P., Brun, E., Morin, S., ... & Peng, S. Evaluation of an improved intermediate complexity snow scheme in the ORCHIDEE land surface model. *Journal of Geophysical Research: Atmospheres*, *118*(12), 6064-6079, 2013.

Weedon, G. P., G. Balsamo, N. Bellouin, S. Gomes, M. J. Best, and P. Viterbo, The WFDEI meteorological forcing data set: WATCH Forcing Data methodology applied to ERA-Interim reanalysis data, Water Resour. Res., 50, 7505–7514, doi:10.1002/2014WR015638, 2014.

Worrall, F., and T. P. Burt. Flux of dissolved organic carbon from U.K. rivers, Global Biogeochem. Cycles, 21, GB1013, doi:10.1029/2006GB002709, 2007.

Worrall F. , Davies H.,  Bhogal A., Lilly A., Evans M.G. , Turner K.,  Burt T.P., Barraclough D. , Smith P. , Merrington G. The flux of DOC from the UK – predicting the role of soils, land use and in-stream losses. J. Hydrol., 448–449, pp. 149-160, 2012.

Yao, Y., Ciais, P., Viovy, N., Li, W., Cresto-Aleina, F., Yang, H., et al. A data-driven global soil heterotrophic respiration dataset and the drivers of its inter-annual variability. *Global Biogeochemical Cycles, 35, 2020 GB006918.* *https://doi.*org/10.1029/2020GB006918, 2021.

Zhang, B., Tian, H., Lu, C., Dangal, S. R. S., Yang, J., and Pan, S.: Global manure nitrogen production and application in cropland during 1860–2014: a 5 arcmin gridded global dataset for Earth system modeling, Earth Syst. Sci. Data, 9, 667–678,

1180    https://doi.org/10.5194/essd-9-667-2017, 2017.

Zhang, H., Lauerwald, R., Regnier, P., Ciais, P., Yuan, W., Naipal, V., ... & Camino-Serrano, M. Simulating erosion-induced soil and carbon delivery from uplands to rivers in a global land surface model. *Journal of advances in modeling earth systems*, *12*(11), e2020MS002121, 2020.

1185    Zhao, M., F. A. Heinsch, R. R. Nemani, and S. W. Running, Improvements of the MODIS terrestrial gross and net primary production global data set, Remote Sens. Environ., 95(2), 164–176, doi:10.1016/j.rse.2004.12.011, 2005.